



A simple ZVI-Fenton pre-oxidation using steel-nails for NOM degradation in water treatment

Naiara O. Dos Santos ^{a, b}, Luiz A.C. Teixeira ^{a, c}, Julio C. Spadotto ^a, Luiza C. Campos ^b  

A simple ZVI-Fenton pre-oxidation using steel-nails for NOM degradation in water treatment

Naiara O. Dos Santos ^{a, b}, Luiz A. C. Teixeira ^{a, c}, Julio C. Spadotto ^a, Luiza C. Campos ^{b*}

^a Department of Chemical and Materials Engineering, PUC-Rio, 22451-900, Rio de Janeiro, Brazil

^b Department of Civil, Environmental and Geomatic Engineering, University College London, London, WC1E 6BT, UK

^c Peroxidos do Brasil Ltda - Solvay Group

* Corresponding author, email: l.campos@ucl.ac.uk

Abstract

The feasibility of a heterogeneous Fenton Process (ZVI/H₂O₂) using commercial low-carbon-steel nails as the Zero-Valent Iron (ZVI) source was evaluated for the first time for the removal of NOM from natural surface waters with distinct physico-chemical characteristics. The synergistic effect of ZVI nails and H₂O₂ on the process was confirmed. Results showed similar removal efficiencies of NOM in water samples from Thames river and Regent's Park lake (both in London, UK) (under initial pH 3.5 and 100% excess of H₂O₂ dosage), reaching dissolved organic carbon (DOC) removals of 61.6% ± 3.0 and 59.6% ± 4.7, and UV₂₅₄ removals of 79.9% ± 0.6 and 77.3 ± 6.2, respectively with 60 min of batch reaction time. ZVI nail surface characterization by scanning electron microscopy (SEM), X-ray energy-dispersive spectroscopy (EDS), and X-ray photoemission spectroscopy (XPS) revealed the formation of a passivating oxide-hydroxide layer on the nail during the reaction, which reduces its surface activity in 20% in continuous use. Results indicate that ZVI/H₂O₂ process using commercial iron nails is a promising pre-oxidation step for drinking water treatment. The low cost of commercial nails together with the facility of separating them from the water are the main advantages for the application of this process in remote regions with limitations in infrastructure and/or finance.

Keywords: Natural organic matter; Natural water; Fenton oxidation; ZVI; iron nail.

1. Introduction

Natural organic matter (NOM) present in waters may be responsible for drinking water quality issues regarding colour, odour, and taste. An additional important concern is the formation of disinfection by-products (DBPs) through the reaction between NOM fractions (mainly hydrophobic portions i.e. humic substances) and the chemicals (mostly chlorine) [1–3] applied for disinfection in water treatment plants (WTPs) [1,4–7].

As well-acknowledged, the DBPs formed in chlorination have generated health concerns such as the increased risk of developing cancer in humans [2,6]. In view of their importance, this issue has been addressed in national standards for drinking water quality in many countries, but if an appropriate treatment is not applied, the presence of NOM in drinking water treatment can cause serious water quality issues [4].

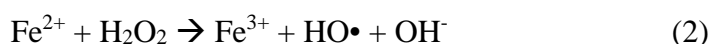
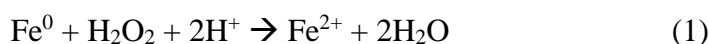
In this context, NOM can pose significant impacts on the efficiency and the cost of water purification [1]. Typically, high concentrations of NOM may increase the required doses of treatment chemicals (such as coagulant and disinfectant) leading to increased sludge formation and dissolved DBPs [3,8,9]. In addition, dissolved NOM causes a challenge for WTPs due to its limited removal in the coagulation, flocculation, and filtration steps [6,7]. According to Bhatnagar and Sillanpää [8], due to the high variability of the NOM, its removal in each of the water purification steps is limited. In this way, several studies aimed at enhancing the efficiency of NOM removal have been carried out [7,10–15], various using Advanced Oxidation Processes (AOPs) with the intent of mineralization [7,16–19]. Some previous investigations using natural water and synthetic water showed average removal of dissolved organic carbon (DOC) around 50 - 60%, using AOPs such as Fenton, photo-Fenton, O₃, UV/H₂O₂, and Electrocoagulation processes [10,20–23]. On the other hand, for efficient mineralization of NOM, some of

these AOPs demand special equipment such as ozone generators, UV lamps and photo-reactors, as well as energy and specialized maintenance [4].

According to Enami et al. [24], there are still controversies regarding the mechanism of Fenton AOP and the identity of the intermediates participating in the oxidative process. The speciation of Fe^{2+} / Fe^{3+} in aqueous solution includes several species of complex ions. The application of some types of metals favoured the formation of a variety of ligated iron (II) complexes in combination with H_2O_2 [25]. Bray and Gorin [26] have proposed a mechanism in which the ferryl ion $[\text{Fe}^{\text{IV}}\text{O}]^{2+}$ may be an active intermediate of the process in addition to other mechanisms based in different active intermediates (such as $\text{HO}\cdot$ and $\text{HOO}\cdot$ radicals). In general, an AOP using ferric (Fe^{+3}) ions or others ions of transition metals in the reaction is named Fenton-like [27]. In the chemistry of both Fenton and Fenton-like reactions, these can occur simultaneously. However, the Fenton-like reaction is weaker than the Fenton one [25,27].

An interesting AOP technology of possible low cost is the heterogeneous ZVI-Fenton process ($\text{ZVI}/\text{H}_2\text{O}_2$), which uses the Zero Valent Iron (ZVI, Fe^0) as a pseudo-catalyst [28] [29]. By way of comparison, typical prices of ZVI powder with 97-99% of purity range from 60-150.0 US\$/kg [30] and range from 0.2-0.6 US\$/kg with 60-98% of purity [31]. Prices of commercial nails can be as low as 5.00 US\$/kg in Brazil and range from 0.30-0.70 US\$/kg [32] in China. In the ZVI process, the metallic iron (Fe^0) is initially corroded in the presence of H_2O_2 (and H^+), oxidating the Fe^0 to Fe^{2+} (Equation (1)), which then reacts with H_2O_2 generating Fe^{3+} and transient reactive oxygen species (ROS), such as the hydroxyl radical ($\text{HO}\cdot$) (Equation (2)). During the reaction, Fe^0 can reduce Fe^{3+} to Fe^{2+} and continue the cycle (Equation (3)). However, depending on the pH, the reduction to Fe^{2+} is not much favoured, as the solubility of Fe^{3+} is more limited in pH closer to neutrality, compared to Fe^{2+} [33, 34]. An also relevant aspect in favour of the $\text{ZVI}/\text{H}_2\text{O}_2$

process is that it is reported that it is successfully used in the degradation of several organic compounds [20, [28,35–39]. According to Fukushima and Tatsumi [40], during the degradation of NOM, the hydrogen abstraction stage in the aromatic sites of the humic fraction may be one of the stages (Equation (4)), resulting in subsequent breaks of the aromatic rings.



The application of less conventional forms of ZVI has been reported in recent years in AOPs. Santos-Juanes et al. [41] investigated the removal of pollutants of emerging concern using steel-wool as source of ZVI to reduce those pollutants. In addition, they employed the iron released in the solution from the ZVI reactions for the photo-Fenton process. Segura et al. [42] evaluated the ZVI/H₂O₂ process on the depuration of a real pharmaceutical wastewater using iron shavings coming from metallurgical residues. Teixeira et al. [43] reported efficiency for phenol removal from ZVI/H₂O₂ process with commercial steel wool as ZVI source. Martins et al. [44] applied iron shavings in ZVI/H₂O₂ process for the remediation of several landfill leachate.

A previous study by the present authors demonstrated the efficiency of the ZVI/H₂O₂ process using a low-cost form of ZVI for removal of NOM and the respective reduction of THM formation [45]. However, to the present authors' knowledge, none of the investigations reported the ZVI/H₂O₂ for degradation of NOM in drinking water treatment using real aquatic matrices with different physico-chemical characteristics. Previous AOPs investigations have reported that the composition of the natural matrix (e.g., the presence of inorganic species such as nitrate, chloride, phosphate, etc.) can

reduce the net supply rate of hydroxyl radical (HO•) [46,47] as these species may act as scavengers. Hence, the overall efficiency of AOPs might be affected due to effect of common raw water matrices' constituents.

Therefore, the aim of the present work was to investigate the heterogeneous ZVI-Fenton process (ZVI/H₂O₂) as a pre-oxidation step in conventional WTPs for the removal of NOM in different surface waters (Thames river and Regent's Park lake, London – UK). This study applied ZVI in the form of small steel-nails to attain simplicity, reduce process costs, and its possible reuse in continuous cycles, which may be especially interesting for WTPs in regions that may lack sufficient infrastructure and/or finance. Also, it is foreseen that in addition to the facility of separation of the nails from the water during the pre-oxidation step [48], the portion of Fe which gets dissolved will be removed as precipitated Fe(OH)₃ in the flocculated sludge.

2. Materials and Methods

2.1 Sampling

The ZVI/H₂O₂ pre-oxidation experiments were performed with water samples from Regent's Park lake (London, UK 51°31'28"N 0°09'15"W) and Thames river (London, UK 51 ° 30'30 "N 0 ° 07'12 "W) [49] collected during the Autumn of 2018 to verify the efficiency of the oxidative process in waters with distinct physico-chemical characteristics. Water samples from the Thames river were collected on 20/11/2018 and had pH = 7.5; weather conditions for that date were precipitation = 3.1 mm and tide state = 3 – 2.5 m [50]. Samples from the Regent's Park lake were also collected during the Summer of 2018 to compare the variation of NOM between Summer and Autumn. Information for Regent's Park lake sampling date and water quality are presented in in Table A.1 (Supplementary Data).

The collected samples (about 6-10 L per collection) were stored at 4°C and used within 4 days in the experiments.

2.2 Materials and chemicals

Hydrogen peroxide (50% w/w) (Solvay) was applied on the experiments from a 1.0 g L⁻¹ stock solution prepared by dilution of 50% concentrated product. All aliquots drawn during runs were quenched with sodium sulfite (Merck, CAS: 7757-83-7) in stoichiometric dosages to extinguish the remaining concentrations of H₂O₂ at the end of the ZVI/H₂O₂ process, according to Liu et al. [51]. All used chemical reagents were of analytical grade and the solutions prepared with ultrapure water (Millipore Milli-Q, resistivity > 18.2 MΩ_{cm}). The ZVI applied in the process was in the form of small low-carbon steel nails (AISI 1010) (ArcelorMittal) with 0.43 cm² g⁻¹ (surface area per gram of each nail). Previous tests performed by Optical Emission Spectroscopy – OES (Spectromax Instrument) [45] showed that the total trace elements contained in the metal amount to only 1% (mass concentration - %) (Table A.2).

2.3 Analytical Procedures

The organic content of the natural water was determined by DOC (TOC-L CPH model TOC analyzer), UV₂₅₄ (Shimadzu UV 1800 spectrophotometer), and specific UV absorbance – SUVA (L mg⁻¹ m⁻¹ = UV₂₅₄/DOC * 100) according to the USEPA Method 415.3 [52] and Standard Methods 5910B [53]. The SUVA₂₅₄ has been one of the parameters applied to correlate the organic matter aromaticity and aquatic humic composition [54,55]. The UV absorbance was measured at 200-400 nm wavelengths to verify the characteristic absorbance of the samples and then, a standard curve was performed at 254 nm, based on previous dilutions of the samples. Calibration curves were performed for each collection and showed R² > 0.9. The determination of nitrate (NO₃⁻),

chloride (Cl^-), phosphate (PO_4^{3-}) and bromide (Br^-) anions of the water matrices was performed using the ion chromatography method (4 mm IonPac AS23 analytical column and the IonPac AG23 guard column). The dissolved Fe^{2+} concentration was measured immediately after removing the aliquots on a HACH 890 colorimeter at 520 nm (10-phenanthroline method adapted from Standard Methods for the Examination of Water and Wastewater) [56–58]. H_2O_2 concentration was monitored on a HACH 890 colorimeter at 420 nm according to Solvay-Peroxidos Brasil's method [59]. Determination of the H_2O_2 concentration was based on the reaction between H_2O_2 and a titanium (IV) salt (Allper reagent, Solvay-Peroxidos Brasil) in an aqueous acidic solution to produce a yellow complex of perititanic acid. After the production of the standard solutions with different concentrations of H_2O_2 and 50 mL of the Allper reagent, a calibration curve was inserted in the HACH 890 photometer, at 420 nm ($R^2 = 0.9964$).

The pH of the water during the experiments was monitored with an interval of 15 min (Mettler Toledo, S47K) and the samples were previously filtered through a 0.45 μm membrane for the analysis.

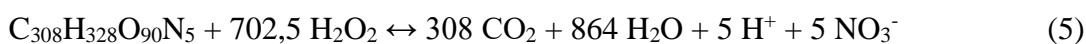
The cross-section of the ZVI-nail specimen was analyzed using field emission gun scanning electron microscopes (FEGSEM) (JEOL JSM 7100F) in secondary electrons (SE) imaging mode operating at 15 kV. X-ray energy dispersive spectroscopy (XEDS), also operated at 15 kV provided qualitative compositional information about the surface deposits on the ZVI, before and after the reaction process. The FEGSEM was equipped with an Oxford Instruments Detector 80 windowless silicon drift detector (SDD). To analyze the cross-section of the ZVI nail, some nails chosen randomly were embedded in resin. Then, the material was subjected to grinding to approximately the center of the nail and, later, it was mechanically polished in diamond paste. The oxides species on the ZVI nail surface before and after ZVI/ H_2O_2 reaction were identified by X-ray photoelectron

spectroscopy (XPS) using spectrometer Thermo K-alpha ($E = 1486.6$ eV). Casa XPS software (version 2.3.16) was used to determine the spectra peaks.

Equipment calibrations were carried out before tests and according to manufacturers' guidelines. The instruments used to performed the characterization of the samples before and during the ZVI/H₂O₂ process are described in the Supplementary Data (Table A.3).

2.4 Experimental Procedure

ZVI/H₂O₂ pre-oxidation experiments were performed under different initial pH conditions (pH 3.5 and 5.5). The stoichiometric dosage of H₂O₂ applied to the natural water was 8.6 mg L⁻¹ per mg L⁻¹ of DOC, based on the Dos Santos' previous study with synthetic water (containing reagent-grade HA) and natural water [60]. In her study, it was assumed that that the H₂O₂ could fully oxidize the HA (with an average molecular weight of the reagent grade HA supplied by Sigma Aldrich) to the extent of full mineralization according to Equation (5). In addition to the consumption of H₂O₂ for ZVI oxidation with consequent generation of aqueous Fe²⁺ ions, it must be acknowledged that the stoichiometric dose considered by this equation does not cover the consumption of H₂O₂ due to possible paralel self-decomposition reactions and consumption of H₂O₂ for oxidation of other dissolved oxidizable species which might be present in natural waters.



Prior to the start of the experiments, the ZVI nails were immersed in a 1% HCl solution (Sigma-Aldrich, CAS: 7647-01-0) for 10 min followed by rinsing (3 times) with distilled water to remove any surface dirt or oxidation. Initially, the pH of the water was adjusted for the subsequent addition of H₂O₂, following re-checking for possible pH adjustments. Once the iron source ZVI was added to the reactor, the reaction time was

initiated (ZVI nails remained static during reactions). Control experiments using only ZVI or only H₂O₂ were also performed. All experiments were carried out under agitation at 250 rpm in jar-test equipment with effective volume of 1 L at room temperature, and aliquots filtered through 0.45 µm syringe filter (Millipore).

Since the objective of this study was to verify the removal of NOM as a preliminary treatment step, the water samples were not subjected to physico-chemical treatments before the processes ZVI/H₂O₂ and control experiments. Table A.4 presents the identification and results of each experiment carried out in this study.

The experiments were carried out in replicates to attest the reproducibility of the results and to estimate the experimental error. Tests with the combined ZVI/H₂O₂ were carried out in triplicates, while tests with only ZVI and H₂O₂ were carried out in duplicates due to water sample volume limitation.

3. Results and Discussion

3.1 Seasonal variation of DOC, UV₂₅₄ and SUVA₂₅₄ concentrations in natural water

Water samples collected from Regent's Park lake during the Summer and Autumn seasons presented variation in their organic content. The values obtained in both seasons were compared at the same collection point. Sample data, such as DOC, UV₂₅₄, pH, temperature and precipitation are shown in Table A.1. As observed in Figure 1, the initial concentrations of DOC and UV₂₅₄ ranged from 2.2 – 7.3 mg L⁻¹ (mean = 4.948 and SD = 1.78) and 0.033 - 0.184 cm⁻¹ (mean = 0.118 and SD = 0.053), respectively. The values of DOC and UV₂₅₄ plotted in Figure A.1 showed determination coefficient R² = 0.9194 with variation of both parameters positively correlated with each

other (Pearson value, $r = 0.9588$). This confirms that the concentrations of DOC and UV_{254} may vary in a similar way. The progressive increase of the DOC and UV_{254} values observed during the Autumn (Figure 1) may be related to the greater fall of vegetation in this season [61].

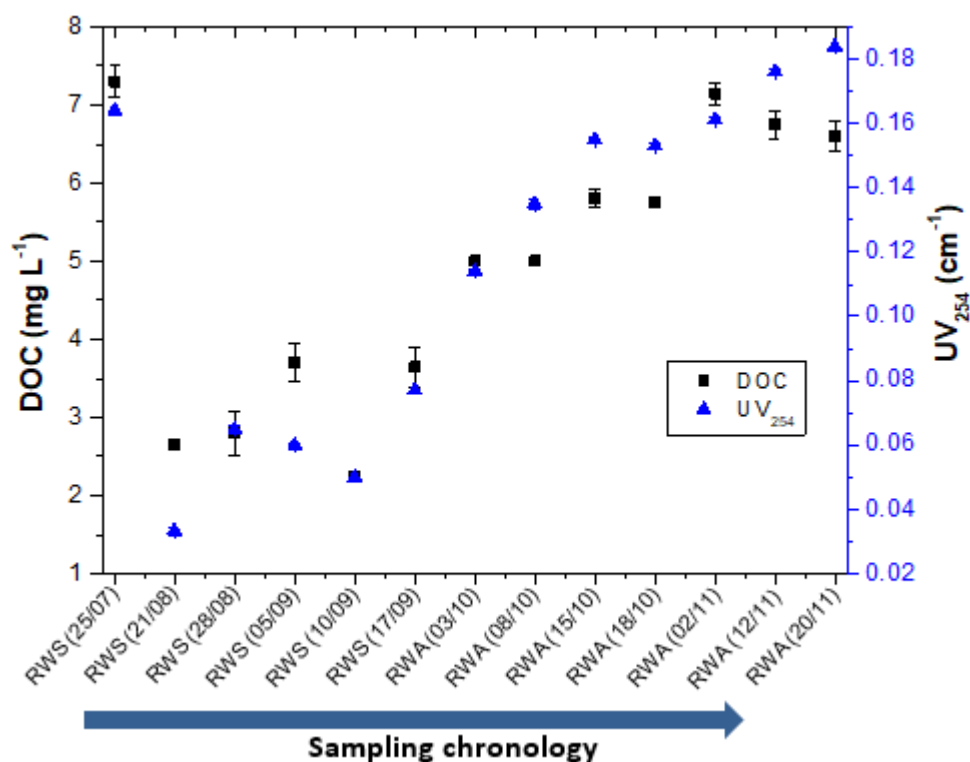


Figure 1 – Variation of DOC and UV_{254} parameters in natural water samples collected in Regent's Park lake during (a) the Summer - RWS and (b) the Autumn – RWA, seasons in 2018.

As a result of the higher amount of fallen vegetation during Autumn compared to Summer, a higher concentration of humic substances due to the biodegradation in this vegetation is expected [8,61]. This is confirmed by the $SUVA_{254}$ values (relation between UV_{254} and DOC parameters) shown in Figure 2. The NOM content with a higher $SUVA_{254}$ value during Autumn ($SUVA_{254} > 2.0 \text{ L mg}^{-1} \text{ m}^{-1}$) may be due to the presence of fractions with higher amounts of aromatic rings [62] and the presence of polyphenols in the leaf material [63,64]. Previous studies suggest that NOM with a high $SUVA_{254}$ value (higher aromatic rings amount) plays an important role in the formation of disinfection by-

products (DBPs), if it reacts with disinfectants such as chlorine [61,65–68]. Therefore, in this study the NOM removal present in natural water was verified from samples collected during the Autumn season.

Changes in both concentration and type of NOM can significantly influence the design and operation of WTPs [8]. In this way, the characteristics of NOM (as $SUVA_{254}$, DOC and UV_{254} parameters) should be taken into account, since the prevention of THM formation in a WTP depends on the removal of different NOM fractions before the disinfection step [65].

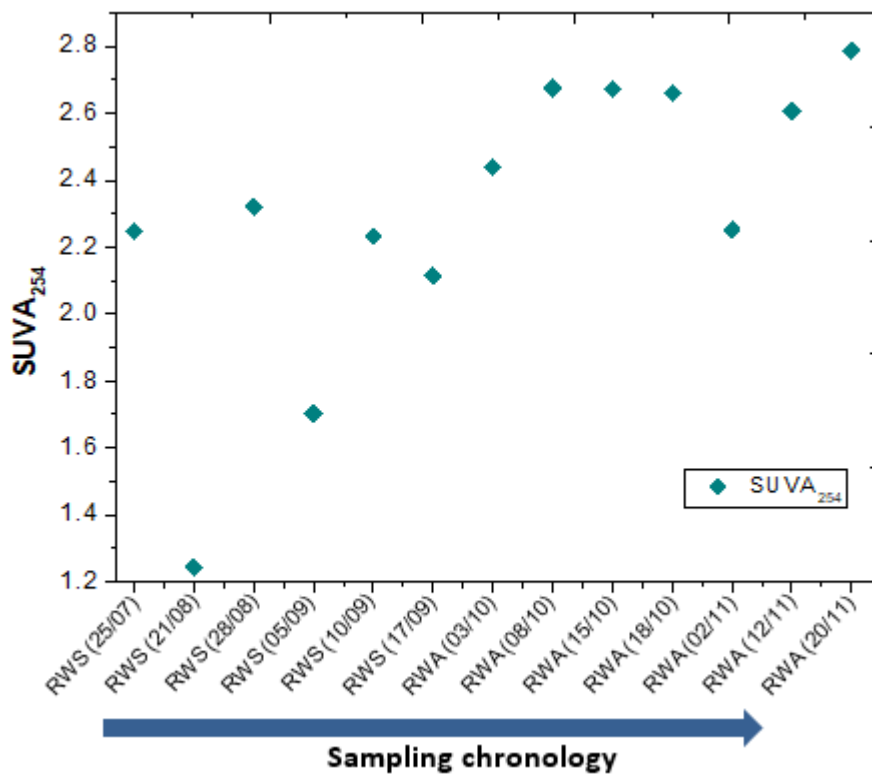


Figure 2 – Variation of $SUVA_{254}$ in natural water samples collected in Regent's Park lake during (a) the Summer - RWS and (b) the Autumn – RWA, seasons in 2018.

3.2 Synergistic Effect of the ZVI and H_2O_2

Results of pre-oxidation experiments performed on water samples from Regent's Park lake collected during the Autumn season (with higher NOM content) were denominated as RWA.

Preliminary experiments to confirm the oxidative effect of the ZVI/H₂O₂ process were performed by applying: 1) only ZVI - samples RWA-10.1 and RWA-10.2; only H₂O₂ - samples RWA-10.3 and RWA-10.4; and 3) both ZVI/H₂O₂ combined reagents - samples RWA-9.1, RWA-9.2 and RWA-9.3 (see Table A.5). The experimental condition was applied according to preliminary tests [60]: pH₀ = 5.5, ZVI = 37.5 g L⁻¹, and [H₂O₂] = 1.5 times the considered stoichiometric amount. The enhanced removal of DOC obtained by the presence of both reagents (i.e. ZVI and H₂O₂) (Figure 3 (a)) confirmed the synergistic effect, which can occur due to the production of oxidative radicals (such as HO•) capable of reacting with the aromatic structure of the organic matter, in agreement with previous works [18,69–71].

Figure 3 (a) shows that the removal of DOC by the ZVI/H₂O₂ process was significantly higher than with only ZVI, with DOC reductions of 28% [45] and 5%, respectively (during 30 min of treatment). However, the calculated data for the rate constants of DOC removal [72,73] by ZVI/H₂O₂ process did not present a satisfactory determination coefficient to affirm that the reaction followed a pseudo-first-order or second order (Table A.6). The comparable reaction using only H₂O₂ (without ZVI) did not show an effect on DOC removal (Figure 3 (a)), confirming previous work that showed that the application of only H₂O₂ does not have significant effect on NOM degradation [18,74]. Figure 3 (b) in the inset of Figure 3 (a) displays the variation of concentration of dissolved Fe⁺² applying only ZVI and ZVI/H₂O₂. The concentration of Fe²⁺ in solution during the ZVI/H₂O₂ process was significantly lower probably due to the presence of H₂O₂, which maintains the iron species oxidized and precipitated as Fe(OH)₃

[16,41]. Results of the pH variation during the reactions using ZVI/H₂O₂, only ZVI and only H₂O₂, are shown in Figure A.2. In Figure 4, it is observed that the concentration of Fe²⁺ applying only ZVI increased to 2.0 mg L⁻¹ in the first 10 min of reaction and decreased continuously afterwards. The continuous decrease of [Fe²⁺] concomitant with the DOC removal (after 15 min) observed in this experiment are caused in part by the precipitation of iron species in the system [75–77] [41]. In addition to the precipitation effect, the continuous aqueous dissolution of O₂ from the air and its action on the surface of the ZVI in the system can coexist [78], which contribute to the observed DOC removal (Equations (6) and (7)).

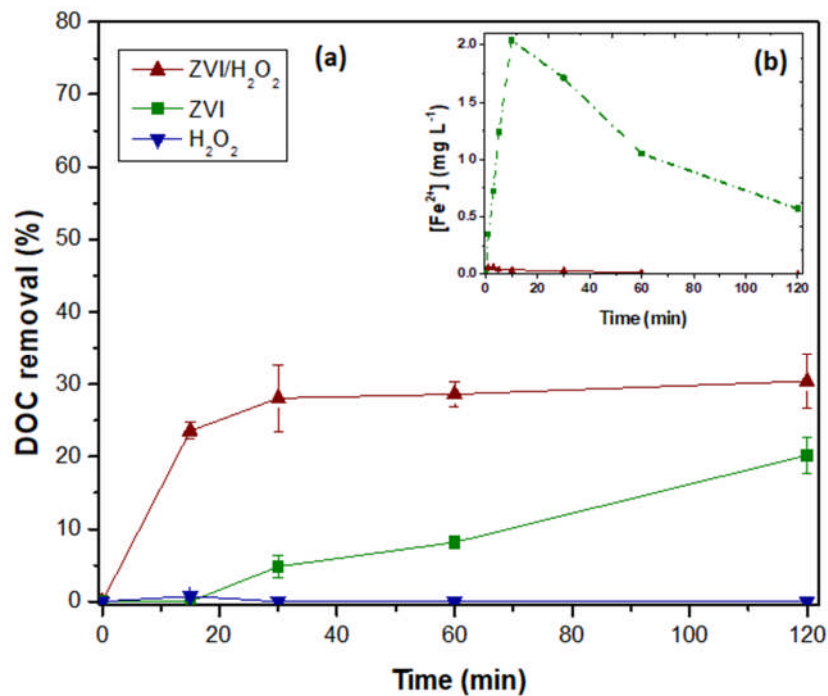
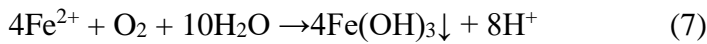
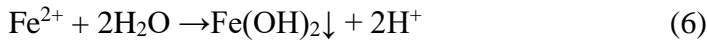


Figure 3 – (a) Removal of DOC by the ZVI/H₂O₂ process (—▲—), by only ZVI nail (—■—), and by only H₂O₂ (—▼—). (b) Concentration of dissolved Fe²⁺ during the ZVI/H₂O₂ process (—▲—) and only ZVI (—■—). Experimental conditions: H₂O₂ = 1.5 times the stoichiometric amount, pH₀ = 5.5, ZVI = 37.5 g L⁻¹. ZVI/H₂O₂

treatment applied in samples RWA-9, n=3 (9.1; 9.2; 9.3). Only ZVI applied in samples RWA-10.1 and RWA-10.2. Only H₂O₂ applied in samples RWA-10.3 and RWA-10.4.

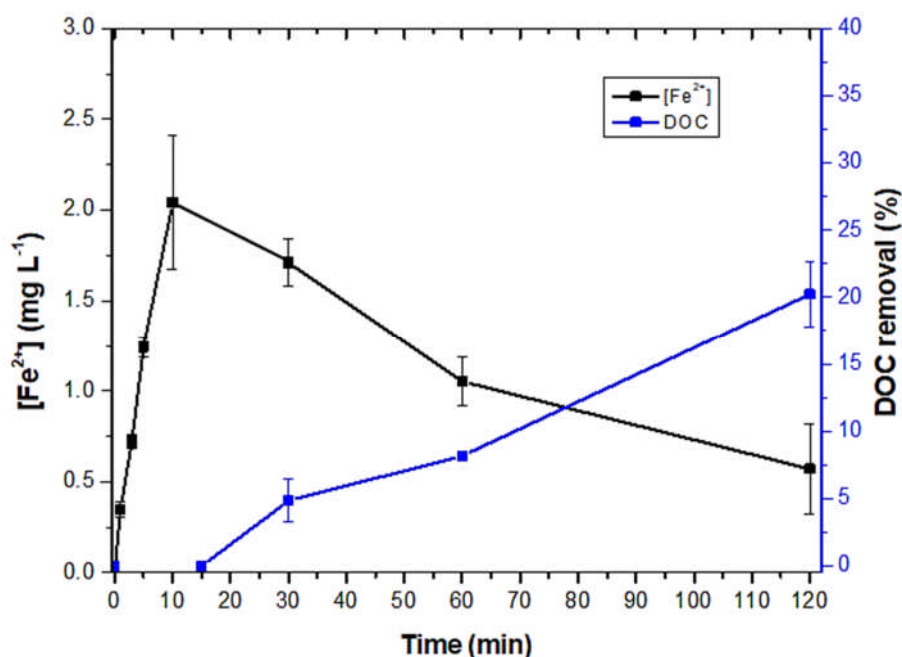


Figure 4 – Formation of Fe²⁺ and removal of DOC during the treatment of the Regent's Park lake water using only ZVI-nail (Samples RWA-10.1 and RWA-10.2). Experimental conditions: pH₀ = 5.5, ZVI nail = 37.5, [H₂O₂] = 1.5 times the stoichiometric amount.

The synergistic effect of ZVI nail and H₂O₂ is also confirmed by comparing the H₂O₂ consumption in both conditions (with and without ZVI) (Figure 5). The results, indicating a substantial consumption of the H₂O₂ when the ZVI is present, are achieved due to the pseudo-catalytic action of ferrous and ferric ions [69,71,79] during the ZVI/H₂O₂ reaction. On the other hand, in the absence of ZVI, the control experiment dosed only with H₂O₂ did not show consumption of the oxidant.

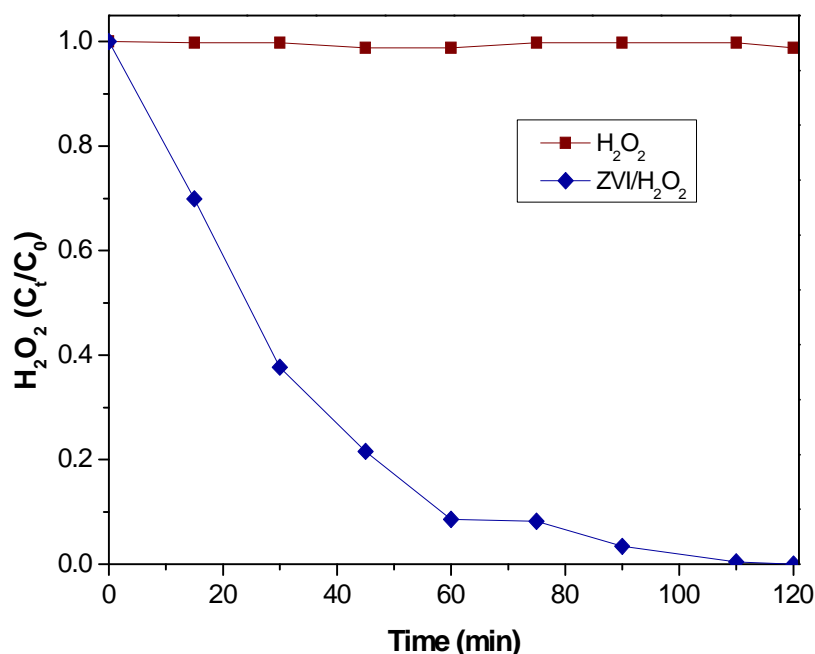


Figure 5 - Decay of the H₂O₂ concentration in Regent's Park samples submitted to the ZVI/H₂O₂ process (—◆—) in samples RWA-9.1, RWA-9.2 and RWA-9.3 and only H₂O₂ (—■—) in samples RWA-10.3 and RWA-10.4. Experimental conditions: pH₀ = 5.5, ZVI nail = 37.5, [H₂O₂] = 1.5 times the stoichiometric amount.

3.5 Application of the ZVI/H₂O₂ process in different surface waters

In order to verify the improvement in the NOM removal through the ZVI/ H₂O₂ process, the initial pH of the process was adjusted to a more acidic range (initial pH = 3.5) [48,80,81].

The ZVI/H₂O₂ treatment (pH₀ = 3.5; ZVI nail = 50 g L⁻¹; [H₂O₂] = 2 times the stoichiometric amount) applied to Regent's Park lake water samples (RWA-12, n=3) for DOC removal showed that the ferrous ions leached to the aqueous solution by the reaction of H₂O₂ and H⁺ ions with the ZVI nail surface provided. This superior catalytic effect on the H₂O₂ consumption was expected [79]. Due to the instability of iron in the presence of water, it will corrode in the presence of an oxidant such as aqueous O₂. Also, the addition of stronger oxidizing agents (such as H₂O₂) to the aqueous medium can increase the

electrochemical potential of the metal corrosion reaction [82], thus favouring the release of Fe^{n+} ions into the water, and their reactions with H_2O_2 in the Fenton mechanism (Equations (1) and (2)). Figure 6 shows that the H_2O_2 consumption and DOC removal occurred mainly in the first 30 min of reaction. After this time, the fairly low (below 5%) remaining H_2O_2 concentration no longer allowed the reaction with ferrous ions to carry on and supply a sufficient rate of $\text{HO}\cdot$ to continue powering the degradation of the DOC. This decrease in DOC removal efficiency may also be related to the formation of oxides on the surface of the ZVI-nail, which can reduce the surface density of reactive sites. The formation of this oxide layer was verified by microscopy analysis and will be further discussed in Section 3.6.

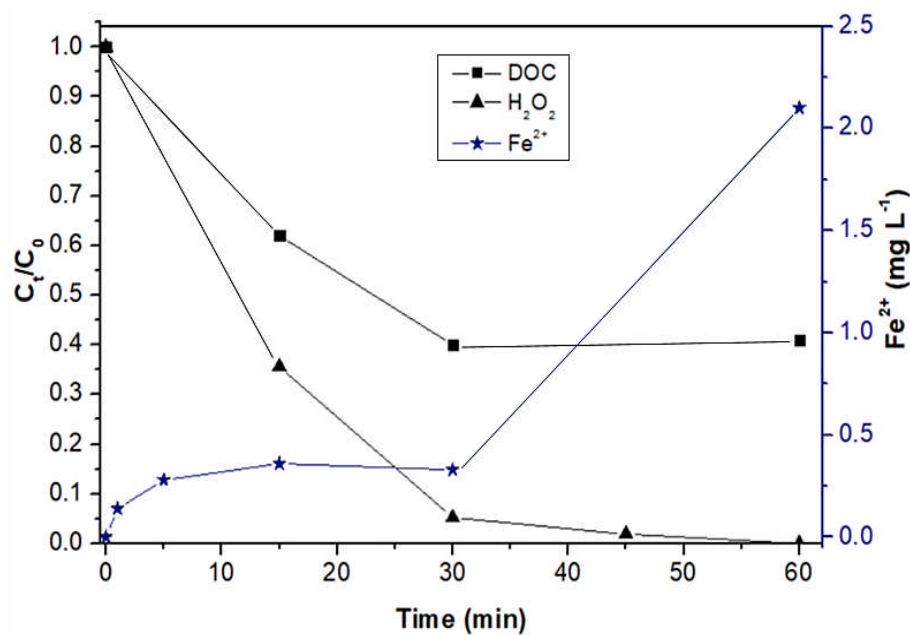


Figure 6 – Variation of H_2O_2 (\blacktriangle) and $\text{Fe}^{2+}_{(\text{aq})}$ (\star) during the ZVI/ H_2O_2 process. NOM removal was evaluated DOC (\blacksquare) parameter. ZVI/ H_2O_2 treatment applied in samples RWA-12.1, RWA-12.2 and RWA-12.3). Experimental conditions: $\text{pH}_0 = 3.5$; ZVI nail = 50 g L^{-1} ; $[\text{H}_2\text{O}_2] = 2$ times the stoichiometric amount.

Water samples from the Thames river were evaluated in order to compare the efficiency of the ZVI/ H_2O_2 process applied to a surface water with different raw

characteristics compared to that of Regent's Park lake water. Thames river is a water body that potentially receives several chemical compounds from domestic, agricultural and industrial discharges [83,84], with tributary watercourses [85], presenting higher exposure to external and anthropogenic factors when compared to Regent's Park lake. Table A.7 shows the different concentrations of inorganic ions present in both surface water samples, indicating higher ion concentration in the Thames river water samples (for example, chloride and nitrate). The UV-Vis spectrum shown in Figure A.3 also indicates differences between Regent's Park lake and Thames river waters. The interference in the Thames river water spectra observed in Figure A.3 is probably due to the presence of chemicals able to absorb light in the 200-400 nm range [86]. The higher values of the parameters seen on the Thames river water may also be due to the location of the sampling point - central London region. Munro et al. [87] identified relevant fluctuations in pharmaceutical and illicit drug residues concentrations in the central London catchment of the Thames river. The authors reported that the pH of the river remained relatively constant over the six weeks ($\text{pH} = 7.77 \pm 0.09$) and conductivity measurements indicated that the river was predominantly composed of freshwater (600–800 μS). Despite being a more central region, smaller changes in ammonium ion concentration and percentage DO were observed across the six-week period. A water characterization study on the Thames river in the Runnymede region (far from the central urban area) reported significantly lower chloride and nitrate concentrations than the present study. However, the concentrations of bromide and DOC were close to those obtained in this study [83]. Water samples collected from Regent's Park lake were used as a study matrix by L.Xu et al. [88]. The characterization of their samples collected during the months of October and November indicated concentrations of DOC and UV_{254} lower than the concentrations obtained in the present study (i.e. $\text{UV}_{254} < 0.095$ and $\text{DOC} < 4.24 \text{ mg L}^{-1}$; $\text{UV}_{254} > 0.122$

and $\text{DOC} > 5 \text{ mg L}^{-1}$, respectively). These concentration differences may be due to the sampling points. Although L.Xu et al. [88] collected water samples in the same Regent's Park lake, the sampling point was located in an area with lower amount of vegetation (location of L.Xu et al.: latitude 51.525187, longitude -0.158017). Nitrate concentrations and turbidity obtained in the present study were also higher than [88].

A previous investigation showed that 2 times the stoichiometric amount of H_2O_2 as optimum dosage when applied in Regent's Park lake water samples [45] for the DOC removal. Experimental results of dosages of H_2O_2 applied to Thames river water from 1 time and 2 times the stoichiometric amount ($\text{pH} = 3.5$ and $\text{ZVI nail} = 50 \text{ g L}^{-1}$) also showed 2 times the stoichiometric amount of H_2O_2 (110 mg L^{-1}) as optimum dosage for DOC removal (Figure A.4). These results agree well with studies that show that as the H_2O_2 dosage increases (to a certain concentration), the rate of generation of $\text{HO}\cdot$ in the reaction medium also increase [71].

As shown in Figure 7, DOC and UV_{254} removals were similar for both water matrices (Regent's Park lake (samples RWA-12) and Thames river (samples TWA-1)) (experimental conditions: $\text{pH}_0 = 3.5$, $[\text{H}_2\text{O}_2]_0 = 2$ times the stoichiometric amount, and $\text{ZVI nail} = 50 \text{ g L}^{-1}$). At 60 min of reaction, the mineralization of DOC was $61.6\% \pm 3.0$ for samples from the Thames river and $59.6\% \pm 4.7$ for samples from Regent's Park lake, with similar H_2O_2 consumption (Equation A.1) in the first 15 min of reaction ($k = 0.069 \text{ min}^{-1}$ and 0.064 min^{-1} for Regent's Park lake and Thames river waters, respectively). The adjustment for the pseudo-first-order reaction model indicated $R^2 = 0.972$ and $R^2 = 0.9389$ for the water from the Regent's Park lake and Thames river, respectively (as shown in Figure A.5). The UV_{254} removal was $79.9\% \pm 0.63$ for Thames river and 77.3 ± 6.2 for Regent's Park lake. These results indicate that the application of the ZVI-nail/ H_2O_2 process on different raw surface waters (without physico-chemical pre- treatments) after

60 min, have a similar NOM removal efficiency, despite the presence of inorganic compounds in different concentrations between both matrices, that can behave as radical scavengers (for example, nitrate, chloride, etc. – see Table A.7) [46]. These results support the possibility of application of the ZVI nail/H₂O₂ process with reasonably good efficiency as a pre-oxidation stage in drinking water treatment.

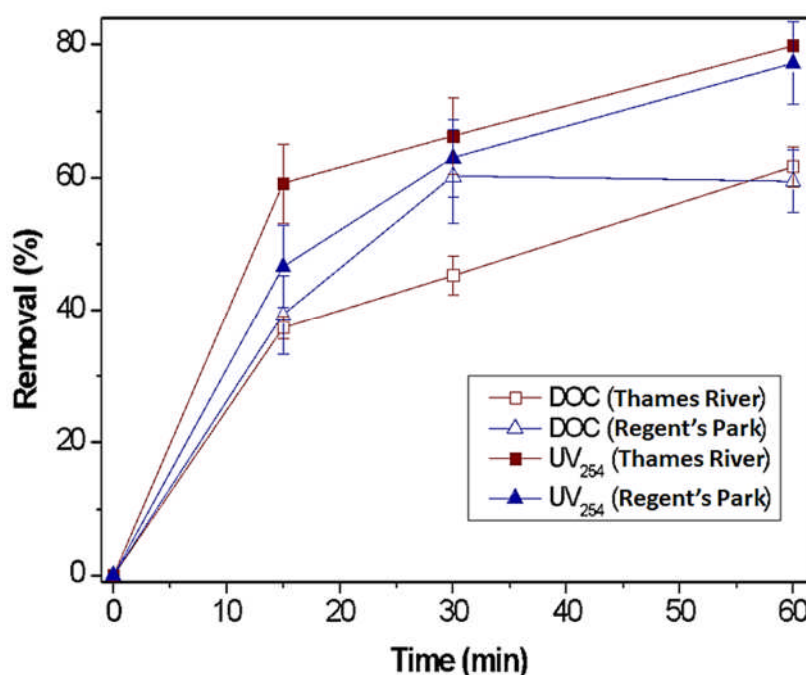


Figure 7 - NOM removal evaluated by DOC and UV₂₅₄ through the ZVI/H₂O₂ process in Thames river (DOC: \square and UV₂₅₄: \blacksquare) and Regent's Park lake (DOC: \triangle and UV₂₅₄: \blacktriangle) waters. ZVI/H₂O₂ treatment applied in Regent's Park lake samples: RWA-12, RWA-12.2 and RWA-12.3. ZVI/H₂O₂ treatment applied in Thames river samples: TWA-1.1, TWA-1.2 and TWA-1.3. Experimental conditions: pH₀ = 3.5, [H₂O₂]₀ = 2 times the stoichiometric amount, and ZVI nail = 50 g L⁻¹.

In addition to the partial DOC mineralization, the significant UV₂₅₄ reduction may indicate that the unsaturated and/or aromatic carbon molecules of the fraction of HA in the NOM were preferentially oxidized [70]. Considering that SUVA₂₅₄ is widely used for estimating the chemical characteristics of DOC (i.e. its aromatic content) [4,52,70], the initial SUVA₂₅₄ values in Regent's Park lake and Thames river waters (initial SUVA₂₅₄ ~

2.5 L mg⁻¹ m⁻¹) indicated NOM structure has a mixture of molecular mass, with intermediate of hydrophobic and hydrophilic [65]. Also, higher initial SUVA₂₅₄ values are expected to be more reactive towards the formation of DBPs [9,65,89]. Thus, as the ZVI/H₂O₂ process favoured the reduction of SUVA₂₅₄ values in both aquatic matrices (SUVA₂₅₄ after treatment = 1.4 ± 0.18 and 1.6 ± 0.5 L mg⁻¹ m⁻¹ for Thames river and Regent's Park lake waters, respectively) a reduction of the aromatic intermediates can be assumed [2,68].

The rates of removal of the inorganic species present in water samples from the Thames river and Regent's Park lake were also observed after 60 min of ZVI/H₂O₂ treatment (Table A.8). The highest removal was of phosphate, reaching 100% of removal for both samples. The range of removals of chloride, nitrate, and bromide analyzed in this study were < 20% in both treated samples. In addition to the formation of Fe-phosphate precipitates, part of the removal of phosphate may be due to adsorption reactions on the surface of the reacted ZVI since the oxide layer formed as a result of the oxidative process can provide active sites for the adsorption of phosphate [90,91]. However, further studies are needed to confirm this adsorption mechanism.

Previous studies using particulate ZVI (without addition of H₂O₂) have also reported good phosphate removal rates (over 80%). However, these studies did not verify the effect of other ions present in the aqueous solution [90,91]. Nagoya et al. [90] evaluated the removal of phosphate in the same pH range as the present study (pH 3-3.5), achieving similar removal efficiency (96% and 100% of phosphate removal for Nagoya et al. and the present study, respectively). However, the authors reported treatment time of 240 min and the process application in a synthetic matrix. It is worth noting that the results of the present study are from different matrices of natural water, in 60 min of treatment.

The ZVI/H₂O₂ process investigated here has the advantage of making use of low-cost commercial nails for removal of NOM in drinking water treatment. Furthermore, previous investigations for NOM and HA removal, such as Fenton, photo-Fenton, O₃, UV/H₂O₂, and Electrocoagulation (applied in natural water and synthetic water) showed lower or similar DOC removal as compared to our study [10,20–23].

3.6 Continued use and Reuse of ZVI nails

The reuse of the ZVI nails on the ZVI/H₂O₂ process using the Regent's Park lake water was evaluated without the application of chemical cleaning/pickling on the ZVI between each run. ZVI was used repeatedly during four cycles of the ZVI/H₂O₂ process. The experiments of the 1st cycle were carried out in triplicate and the others in duplicate, under the conditions of pH₀ = 3.5, [H₂O₂] = 2 times the stoichiometric amount, and ZVI = 50 g L⁻¹. Figure 8 shows a decrease in the removals of DOC and UV₂₅₄ after the 1st cycle (DOC removal: 59.6% ± 4.7 and UV₂₅₄ removal: 77.3% ± 6.2 - samples RWA-12.1, RWA-12.2 and RWA-12.3) and stability in their removal between the 3rd and 4th cycles (DOC removal: 41.5% ± 4.9 in the 3rd cycle and 38% ± 5.7 in the 4th cycle. UV₂₅₄ removal: 66.3% ± 2.4 in the 2nd cycle, 60% ± 3.5 in the 3rd cycle and, 60.6% ± 4.9 in the 4th cycle). The results of removing DOC in the 2nd cycle are not presented due to a technical problem in the equipment.

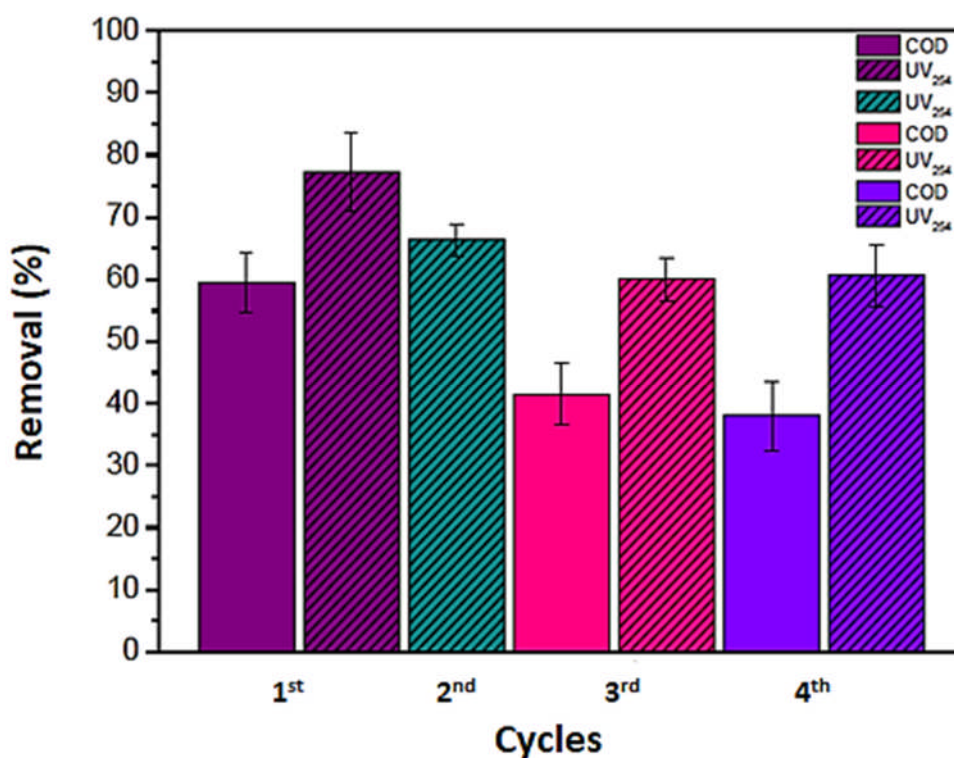


Figure 8 – Effect of reuse cycles of the ZVI nails application in the ZVI/H₂O₂ process for NOM removal evaluated by DOC and UV₂₅₄ from Regent's Park lake water samples (RWA-12). Experimental conditions: pH₀ = 3.5, [H₂O₂]₀ = 2 times the stoichiometric amount, and ZVI nail = 50 g L⁻¹.

It is known that the presence of H₂O₂ in contact with the ZVI surface and the presence of DO initiates a series of reactions to form oxides [92], and these oxides can participate in different ways in the mechanism of the Fenton reaction. However, it is still difficult to determine the extent of its influence on the process [93]. The decrease in H₂O₂ consumption during the ZVI used in each cycle (Figure 9) corroborates the lower DOC and UV₂₅₄ removals observed in this study. Based on these observations, it can be proposed that as the ZVI nail was reused, thickening of the oxy-hydroxides layer occurred [28,48,94], reducing the surface density of reactive sites and, consequently, the rate of H₂O₂ consumption [44,95].

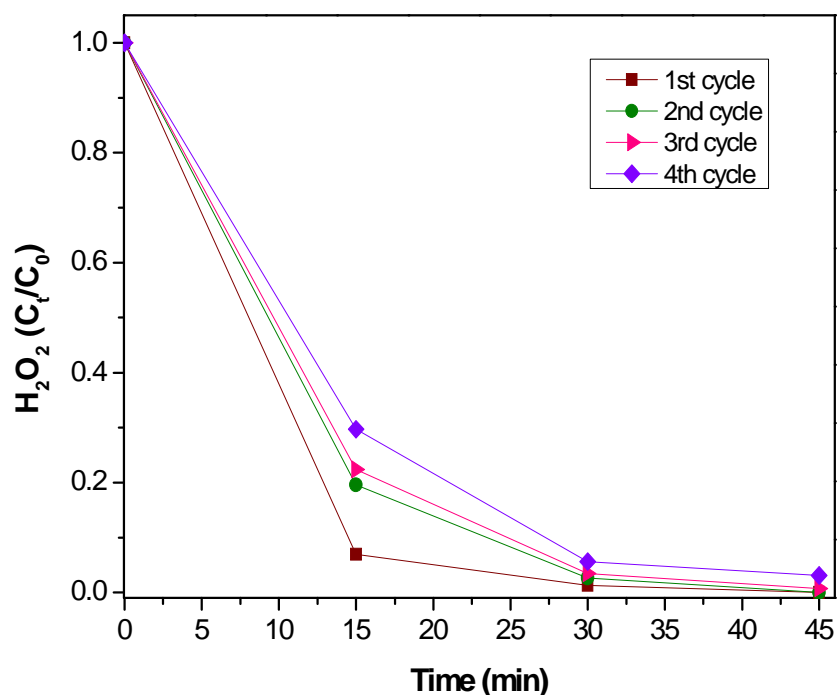


Figure 9 - Decay of the H_2O_2 concentration on the ZVI/ H_2O_2 process from the four cycles of ZVI reuse. Experimental conditions: $\text{pH}_0 = 3.5$, $[\text{H}_2\text{O}_2]_0 = 2$ times the stoichiometric amount), and ZVI nail = 50 g L^{-1} .

The formation of this passive layer during the ZVI/ H_2O_2 process was confirmed through the results of SEM/EDS obtained in the cross-section of the ZVI nail, as shown in Figure 10. Figure 10 (a - b) shows secondary electrons (SE)-SEM images and corresponding XEDS maps of Fe and O obtained from the nail before and after the 1st cycle, respectively. It is observed in Figure 10 (b) an oxide layer formed during the ZVI/ H_2O_2 process, which is confirmed by EDS results that indicate a predominant presence of O in this layer (this observation was consistent in this investigation).

XPS analyses on ZVI nail surface before and after ZVI/ H_2O_2 process shown in Figure 11 (a - c) supported the idea of the existence of an oxide layer formed during the process and confirm the results obtained from the SEM/EDS. Figure 11 (a) shows a lower peak in the O 1s spectrum (peaked at 529.9 eV) attributed to Fe-O [96,97] before the ZVI

nail use on the 1st cycle. After the 1st and 2nd cycles (Figure 11 (b - c)), a progressive increase in peak (binding between O and Fe) is observed, indicating that during the ZVI/H₂O₂ process occurred the formation of an oxide layer on the ZVI nail surface. Also, the characterization of the valence state of Fe from XPS scan on the surface of the ZVI nail before and after the 1st and 2nd cycles of application was obtained (Figure 12). The bonding energy positions Fe 2p_{3/2} and Fe 2p_{1/2} were 711.4 and 724.8 eV, respectively, corresponding to the Fe (III) species [28,91,98,99]. A progressive increase in the intensity of the peaks was observed after the 1st cycle of ZVI nail application. However, the same was not observed after the 2nd cycle, indicating the stability of the formation/deposition of Fe (III) species on the surface of the reacted iron.

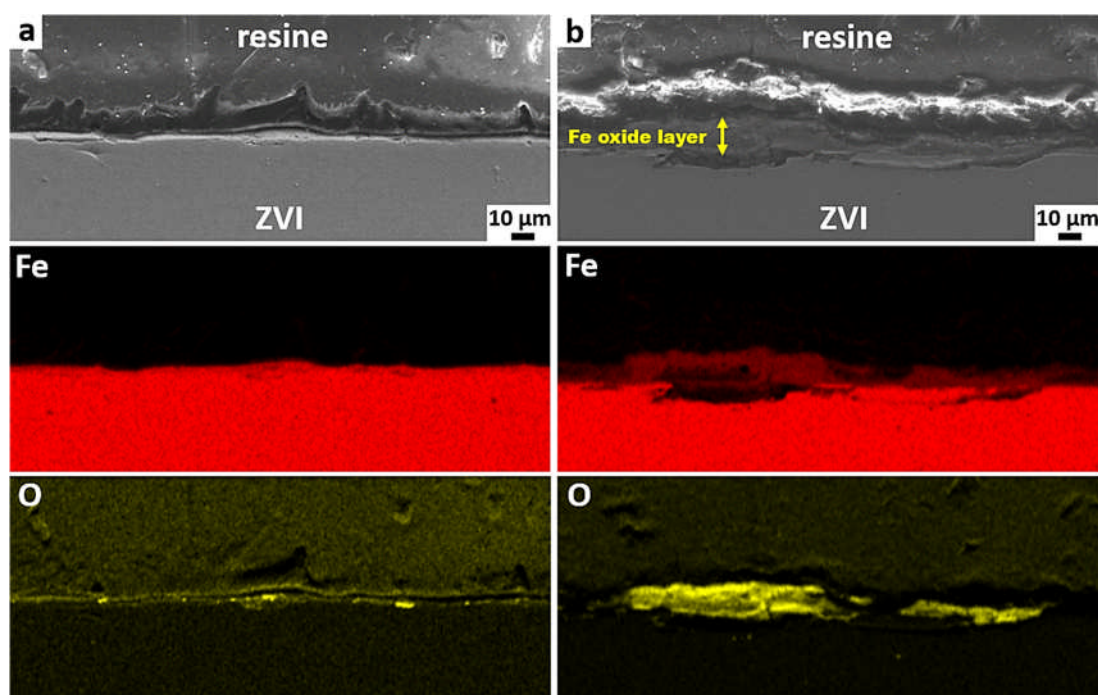


Figure 10 - Cross-sectional images by SEM of the ZVI nail (a) before and (b) after the 1st cycle of the ZVI/H₂O₂ process and corresponding EDS maps of Fe and O. (a) EDS maps shows the predominance of the Fe element. (b) oxide layer of iron oxides is observed on the surface of the reacted ZVI nail. Experimental conditions: pH₀ = 3.5, [H₂O₂]₀ = 2 times the stoichiometric amount, and ZVI nail = 50 g L⁻¹.

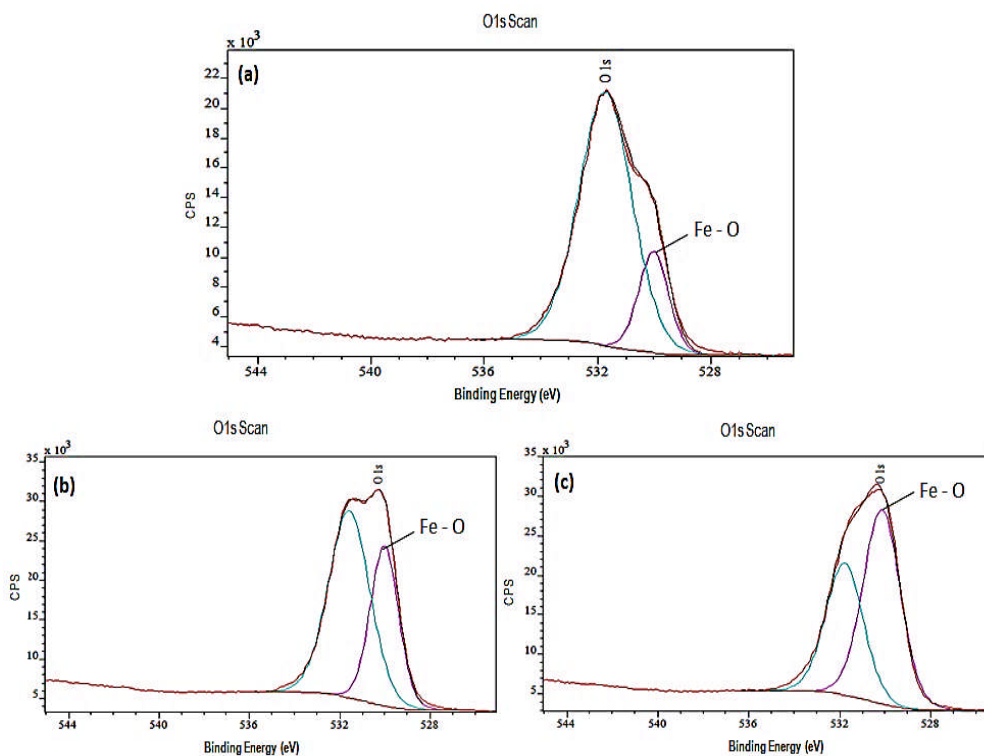


Figure 11 – XPS spectrum obtained from the ZVI nail samples (a) before ZVI/H₂O₂ reaction (b) after the 1st cycle of the ZVI/H₂O₂ reaction and (c) after the 2nd cycle of the ZVI/H₂O₂ reaction. Experimental conditions: pH₀ = 3.5, ZVI = 50 g L⁻¹, [H₂O₂] = 2 times the stoichiometric amount.

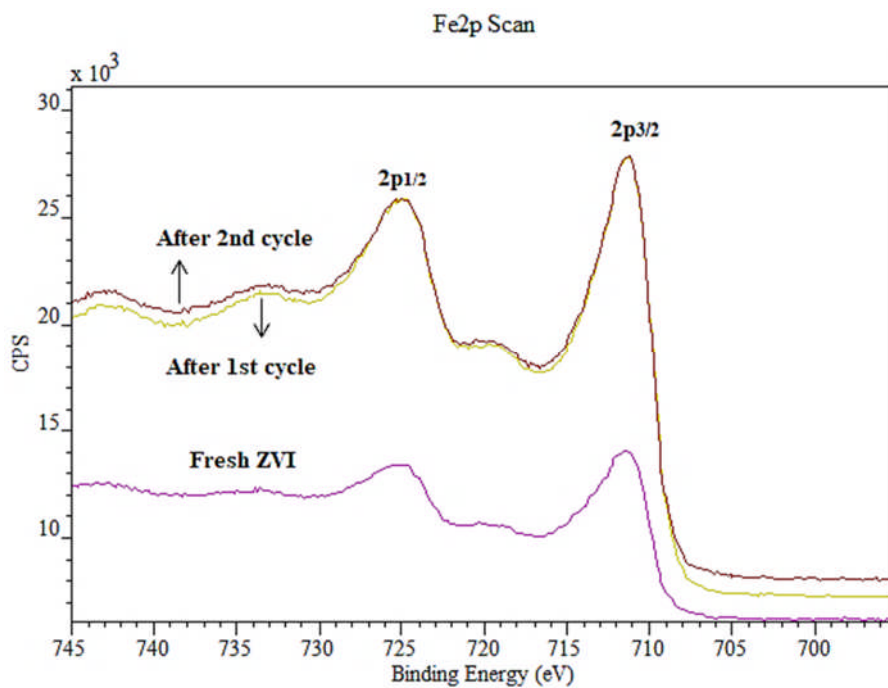


Figure 12 - XPS spectroscopy of the ZVI nail before and after the 1st and 2nd ZVI use cycle in the ZVI/H₂O₂ process. Experimental conditions: pH₀ = 3.5, [H₂O₂]₀ = 2 times the stoichiometric amount, and ZVI = 50 g L⁻¹.

Based on these results, it can be considered that the exposed surface area of the ZVI nail available for reaction with H₂O₂ (and H⁺ ions) has been progressively reduced and replaced by oxo-hydroxide species. These oxides may constitute the formation of a passive layer on the metal [44,75,100], hindering Fe dissolution, thus decreasing the degradation rate of NOM as the ZVI nail is reused in a new cycle. However, a stability effect of this oxide layer after the 2nd cycle of the ZVI nail reuse can also be speculated. As shown in Figure 8, the removal rates of DOC and UV₂₅₄ remained constant during the 3rd and 4th reuse cycles.

A previous work [44] reported that the use of ZVI cuts in ZVI/H₂O₂ for the treatment of urban landfill leachate (after the biological treatment stage) showed decrease of the efficiency of the process from 60% to 42% after the 4th cycle. The reuse of ZVI particles in another study of ZVI/H₂O₂ for the removal of chemical oxygen demand (COD) in citric acid effluent [28] showed an increase in the removal after the 1st cycle of ZVI use (removal of 30% in the 1st cycle, and 45% in the 2nd cycle) followed by a continuous decline (38% removal in the 4th cycle and 7% in the 7th cycle). In our study, despite the observed decrease of about 20% in the efficiency of the process, tending to stabilize at the end of the 4th cycle of reuse of the ZVI nails, the obtained results are promising from the point of view of the applicability of the steel nails in ZVI/H₂O₂. The rate of the overall pre-oxidation reaction may be tuned in accordance with how much surface area of nails is continuously maintained (as surface-oxidized (passivated) iron nails) in the pre-oxidation reactor.

3.7 Overall remarks about the application of ZVI Fenton pre-oxidation

Generally, the cost of chemicals is considered to be responsible for the largest expenses in Fenton's process [101]. In this work, the cost of reagents were based on the experimental conditions presented in Sections 3.5 and 3.6. The costs of the reagents to adjust the pH were considered secondary [102]. At the end of 60 min, the pH of water treated reached ~5.0 for Thames river and Regent's Park lake water samples (Figure A.6). Hence, the demand of the reagent to adjust the pH (i.e. NaOH) for the subsequent coagulation/flocculation steps will be low. The average unitary price of H₂O₂ (100% basis, according to the current average price: ~ 800 US\$/ton) was used to calculate the cost of the reagent per one cubic meter of water, according to Rodriguez et al.'s equation [102]. The average cost of H₂O₂ obtained was 0.21 US\$/m³. The H₂O₂ cost in the AOP can vary due to mainly two reasons: (a) the range of mineralization of the target-pollutant [103,104] and (b) the aquatic study matrix - considering that the H₂O₂ demand for abatement of the NOM of the water matrices of the present study could be lower than the demand required for other organic compounds present in industrial wastewater, for example. The cost of the iron nails has a greater price variation depending on the region. Costs in Brazil (where carbon steel nails were purchased: 2.3 – 5.4 US\$/kg) [105,106] and China (0.35 – 0.70 US\$/kg) [32] are significantly lower compared to UK (~ 16.0 US\$/kg) [107] (price comparison based on similar size and composition of nails). Even with this regional variation of the prices, it should be considered that the consumption of iron nails in a continuous operation is limited to re-stocking the amount of Fe that is dissolved from the nails during the reaction. Actual possible modes of contacting the water with the iron nails in a full-scale operation could be defined by using open tanks filled with nails in a static fixed bed through which water passes through during a preset contact time. Also, the patents by Anderson (1883) [108] in which a revolving reactor

was used, and other patents that ensued, describe potential reactors. Insoluble $\text{Fe}(\text{OH})_3$ precipitates that are also expected to form during pre-oxidation may be removed during flocculation and sedimentation steps. As with any proposed process, pilot-scale and full-scale trials will be necessary in future investigations to better evaluate the total treatment costs, with further tests done with larger number of replicates.

It may also be suggested that tests using a control ZVI-nail sample should be mechanically or acidically cleansed between batches to compare with results showed in this work. In addition, for a better understanding of the oxidative process, it is suggested to investigate the possible influence of HA and/or FA in the NOM as electron shuttle mediators during the process.

4. Conclusions

- The ZVI/ H_2O_2 Fenton pre-oxidation process studied here showed significant effectiveness and similar efficiencies for NOM removal in real water matrices with different physico-chemical characteristics (Regent's Park lake and Thames river, London, UK). Significant NOM removals were reached, with DOC and UV_{254} removals up to 61% and 80%, respectively, in 60min of batch treatment time with 100% of excess over the considered stoichiometric amount of H_2O_2 and initial pH adjusted to pH 3.5.
- The ZVI employed in the form of small carbon steel nails was able to perform as a pseudo-catalyst, functioning as a source of Fe^{n+} ions, confirming its reactivity in the ZVI/ H_2O_2 Fenton process.
- A passive oxide layer formed during the ZVI/ H_2O_2 process was identified and pointed as one of the responsible causes for reducing the concentration of reactive

Fe sites on the ZVI nail surface. As the ZVI nail was reused in a sequence of 4 batch runs of 1 h each, a reduction of NOM degradation of around 20% compared with the degradation obtained by new nails was observed, but that was seen to stabilize at the end of the 4 hours. As the Fenton-ZVI reaction rate depends on the surface area of the pseudo-catalyst, in a continuous operation it will be possible to control the speed of the overall reaction by adjusting the amount/surface of nails maintained in the pre-oxidation reactor so the surface passivation that occurs does not hinder the performance of the process.

- The low cost of the pseudo-catalyst material in the form of nails (up to 1,000 US\$/ton), their wide commercial availability, and the lack of need for specialized equipment make this AOP attractive as a pre-oxidation step in WTPs for remote regions with limitations in infrastructure and/or finance.

Acknowledgements

The authors are gratefully Dr. R. G. Palgrave of the University College London - Department of Chemistry for XPS analyses and technical support, advice, assistance and LABNANO/CBPF for technical support during electron microscopy work. The Royal Parks are acknowledged for authorising the water collection from the Regent's Park lake.

Funding

Naiara de Oliveira dos Santos acknowledges her doctoral scholarship supported by the Brazilian Agencies: Coordenação de Aperfeiçoamento de Pessoal de Nível Superior (CAPES), Conselho Nacional de Desenvolvimento Científico e Tecnológico (CNPq), and Fundação Carlos Chagas Filho de Amparo à Pesquisa do Estado do Rio de Janeiro (FAPERJ) (DSC10-01/2018).

Conflict of Interest Statement

The authors declare that they have no conflict of interest.

Credit Author Statement

Naiara de Oliveira dos Santos: Conceptualization, Methodology, Investigation, Writing-Original Draft; **Luiz A. C. Teixeira:** Conceptualization, Funding Acquisition, Writing-Review and Editing, Supervision; **Julio C. Spadotto:** Microscopy analysis, Writing-Review; **Luiza C. Campos:** Conceptualization, Project Administration, Writing-Review and Editing, Supervision.

References

- [1] Richardson SD, Plewa MJ, Wagner ED, et al. Occurrence, genotoxicity, and carcinogenicity of regulated and emerging disinfection by-products in drinking water: A review and roadmap for research. *Mutat Res - Rev Mutat Res.* 2007;636:178–242.
- [2] Fu J, Lee W, Coleman C, et al. Removal of disinfection byproduct (DBP) precursors in water by two-stage biofiltration treatment. *Water Res.* 2017;123:224–235.
- [3] Jo CH, Dietrich AM, Tanko JM. Simultaneous degradation of disinfection byproducts and earthy-musty odorants by the UV/H₂O₂ advanced oxidation process. *Water Res.* 2011;45:2507–2516.
- [4] Tak S, Vellanki BP. Natural organic matter as precursor to disinfection byproducts and its removal using conventional and advanced processes: state of the art review. *J Water Health.* 2018;16:681–703.
- [5] Krasner SW, Weinberg HS, Richardson SD, et al. Occurrence of a new generation of disinfection byproducts. *Environ Sci Technol.* 2006;40:7175–7185.
- [6] Karanfil T, Krasner SW, Westerhoff P, et al. Disinfection By-Products in Drinking Water: Occurrence, Formation, Health Effects, and Control. Karanfil T, Krasner SW,

- Westerhoff P, et al., editors. Washington, DC: American Chemical Society; 2008.
- [7] Sillanpää M. Natural Organic Matter in Water: Characterization and Treatment Methods [Internet]. First Edit. IWA Pub, editor. Finland: Elsevier; 2015. Available from: <https://linkinghub.elsevier.com/retrieve/pii/C20130192136>.
- [8] Bhatnagar A, Sillanpää M. Removal of natural organic matter (NOM) and its constituents from water by adsorption – A review. *Chemosphere*. 2017;166:497–510.
- [9] Kristiana I, Tan J, McDonald S, et al. Characterization of the Molecular Weight and Reactivity of Natural Organic Matter in Surface Waters. In: ACS Symposium Series, editor. *Adv Physicochem Charact Dissolved Org Matter Impact Nat Eng Syst*. 2014. p. 209–233.
- [10] McBeath ST, Mohseni M, Wilkinson DP. Pilot-scale iron electrocoagulation treatment for natural organic matter removal. *Environ Technol*. 2020;41:577–585.
- [11] Rasheed S, Campos LC, Kim JK, et al. Optimization of total trihalomethanes' (TTHMs) and their precursors' removal by granulated activated carbon (GAC) and sand dual media by response surface methodology (RSM). *Water Sci Technol Water Supply*. 2016;16:783–793.
- [12] Kim JK, Jang DG, Campos LC, et al. Synergistic Removal of Humic Acid in Water by Coupling Adsorption and Photocatalytic Degradation Using TiO₂/Coconut Shell Powder Composite. *J Nanomater*. 2016;2016.
- [13] Matilainen A, Vepsäläinen M, Sillanpää M. Natural organic matter removal by coagulation during drinking water treatment: A review. *Adv Colloid Interface Sci*. 2010;159:189–197.
- [14] Xia S, Ni M. Preparation of poly(vinylidene fluoride) membranes with graphene oxide addition for natural organic matter removal. *J Memb Sci*. 2015;473:54–62.
- [15] Zhao Y, Li N, Xia S. Polyamide nanofiltration membranes modified with Zn–Al layered double hydroxides for natural organic matter removal. *Compos Sci Technol*. 2016;132:84–92.
- [16] Katsumata H, Sada M, Kaneco S, et al. Humic acid degradation in aqueous solution by

- the photo-Fenton process. *Chem Eng J.* 2008;137:225–230.
- [17] Rodríguez FJ, Schlenger P, García-Valverde M. A comprehensive structural evaluation of humic substances using several fluorescence techniques before and after ozonation. Part I: Structural characterization of humic substances. *Sci Total Environ.* 2014;476–477:718–730.
- [18] Lamsal R, Walsh ME, Gagnon GA. Comparison of advanced oxidation processes for the removal of natural organic matter. *Water Res.* 2011;45:3263–3269.
- [19] Uyguner CS, Bekbolet M. Contribution of metal species to the heterogeneous photocatalytic degradation of natural organic matter. *Int J Photoenergy.* 2007;2007.
- [20] Murray CA, Parsons SA. Removal of NOM from drinking water: Fenton's and photo-Fenton's processes. *Chemosphere.* 2004;54:1017–1023.
- [21] Cui Y, Yu J, Su M, et al. Humic acid removal by gas-liquid interface discharge plasma: performance, mechanism and comparison to ozonation. *Environ Sci Water Res Technol.* 2019;5:152–160.
- [22] Sarathy S, Mohseni M. Effects of UV/H₂O₂ advanced oxidation on chemical characteristics and chlorine reactivity of surface water natural organic matter. *Water Res.* 2010;44:4087–4096.
- [23] Moncayo-Lasso A, Rincon AG, Pulgarin C, et al. Significant decrease of THMs generated during chlorination of river water by previous photo-Fenton treatment at near neutral pH. *J Photochem Photobiol A Chem.* 2012;229:46–52.
- [24] Enami S, Sakamoto Y, Colussi AJ. Fenton chemistry at aqueous interfaces. *Proc Natl Acad Sci [Internet].* 2014;111:623–628. Available from: <http://www.pnas.org/cgi/doi/10.1073/pnas.1314885111>.
- [25] Ensing B, Buda F, Baerends EJ. Fenton-like Chemistry in Water: Oxidation Catalysis by Fe(III) and H₂O₂. *J Phys Chem A.* 2003;107:5722–5731.
- [26] Bray WC, Gorin MH. FERRYL ION, A COMPOUND OF TETRAVALENT IRON. *J Am Chem Soc.* 1932;54:2124–2125.
- [27] Jiang C, Pang S, Ouyang F, et al. A new insight into Fenton and Fenton-like processes

- for water treatment. *J Hazard Mater* [Internet]. 2010;174:813–817. Available from: <https://linkinghub.elsevier.com/retrieve/pii/S0304389409015866>.
- [28] Huang T, Zhang G, Zhang N, et al. Fe⁰-H₂O₂ for advanced treatment of citric acid wastewater: Detailed study of catalyst after several times use. *Chem Eng J*. 2018;336:233–240.
- [29] Nidheesh P V. Heterogeneous Fenton catalysts for the abatement of organic pollutants from aqueous solution: a review. *RSC Adv*. 2015;5:40552–40577.
- [30] Sigma-Aldrich. Iron Powder - Sigma-Aldrich USA. 2020. p. 1–6.
- [31] Iron Powder For Powder Metallurgical Products - prices [Internet]. 2021 [cited 2018 Mar 17]. p. 1–5. Available from: https://www.alibaba.com/product-detail/High-Quality-Reduced-Iron-Powder-for_62314378311.html?spm=a2700.7724857.
- [32] Hebei Qunkun Metal Products Co. L. Steel Carbon Steel Nail [Internet]. 2021 [cited 2021 Mar 21]. p. 1–16. Available from: <https://m.made-in-china.com/product/45-Steel-Carbon-Steel-Cement-Nail-759706322.html>.
- [33] Litter MI, Slodowicz M. An overview on heterogeneous Fenton and photoFenton reactions using zerovalent iron materials. *J Adv Oxid Technol*. 2017;20.
- [34] Chakinala AG, Bremner DH, Burgess AE, et al. A modified advanced Fenton process for industrial wastewater treatment. *Water Sci Technol*. 2007;55:59–65.
- [35] Bremner DH, Burgess AE, Houlemare D, et al. Phenol degradation using hydroxyl radicals generated from zero-valent iron and hydrogen peroxide. *Appl Catal B Environ*. 2006;63:15–19.
- [36] Wu Y, Zhou S, Qin F, et al. Modeling the oxidation kinetics of Fenton's process on the degradation of humic acid. *J Hazard Mater*. 2010;179:533–539.
- [37] Molnar JJ, Agbaba JR, Dalmacija BD, et al. A study on the removal of natural organic matter and disinfection byproducts formation potential from groundwater using Fenton's process. *J Adv Oxid Technol*. 2011;14:54–62.
- [38] Jung HJ, Hong JS, Suh JK. A comparison of fenton oxidation and photocatalyst reaction efficiency for humic acid degradation. *J Ind Eng Chem*. 2013;19:1325–1330.

- [39] Aftab B, Shin H-S, Hur J. Exploring the fate and oxidation behaviors of different organic constituents in landfill leachate upon Fenton oxidation processes using EEM-PARAFAC and 2D-COS-FTIR. *J Hazard Mater* [Internet]. 2018;354:33–41. Available from: <https://linkinghub.elsevier.com/retrieve/pii/S0304389418303091>.
- [40] Fukushima, M. and Tatsumi K. Degradation Characteristics of Humic Acid during Photo-Fenton Processes. *Environ Sci Technol*. 2001;35:3683–3690.
- [41] Santos-Juanes L, García Einschlag FS, Amat AM, et al. Combining ZVI reduction with photo-Fenton process for the removal of persistent pollutants. *Chem Eng J*. 2017;310:484–490.
- [42] Segura Y, Martínez F, Melero JA. Effective pharmaceutical wastewater degradation by Fenton oxidation with zero-valent iron. *Appl Catal B Environ*. 2013;136–137:64–69.
- [43] Teixeira LAC, Vieira NDA, Yokoyama L, et al. Degradation of phenol in mine waters using hydrogen peroxide and commercial steel wool. *Int J Miner Process*. 2015;138:15–19.
- [44] Martins RC, Lopes D V., Quina MJ, et al. Treatment improvement of urban landfill leachates by Fenton-like process using ZVI. *Chem Eng J*. 2012;192:219–225.
- [45] dos Santos N de O, Teixeira LA, Zhou Q, et al. Fenton pre-oxidation of natural organic matter in drinking water treatment through the application of iron nails. *Environ Technol*. 2021;1–14.
- [46] Lado Ribeiro AR, Moreira NFF, Li Puma G, et al. Impact of water matrix on the removal of micropollutants by advanced oxidation technologies. *Chem Eng J*. 2019;363:155–173.
- [47] Bouasla C, Ismail F, Samar ME-H. Effects of operator parameters, anions and cations on the degradation of AY99 in an aqueous solution using Fenton's reagent. Optimization and kinetics study. *Int J Ind Chem*. 2012;3:15.
- [48] Wang N, Zheng T, Zhang G, et al. A review on Fenton-like processes for organic wastewater treatment. *J Environ Chem Eng*. 2016;4:762–787.
- [49] U.S. Department of the Interior. Earth Explorer [Internet]. 2021 [cited 2021 Mar 8]. p.

2021. Available from: <https://earthexplorer.usgs.gov/>.
- [50] National Environment Agency; NEA. Tide Times [Internet]. 2013 [cited 2021 Mar 18]. p. 1–24. Available from: <http://app2.nea.gov.sg/home-lite/weather-lite/tide-information>.
- [51] Liu W, Andrews SA, Stefan MI, et al. Optimal methods for quenching H₂O₂ residuals prior to UFC testing. *Water Res.* 2003;37:3697–3703.
- [52] USEPA. Method 415.3. Determination of Total Organic Carbon and Specific UV Absorbance at 254 nm in Source Water and Drinking Water. Ohio; 2009.
- [53] Introduction A. 5910 UV-ABSORBING ORGANIC CONSTITUENTS * 5910 B . Ultraviolet Absorption Method. *Water.* 2000;3:71–74.
- [54] Gumus D, Akbal F. A comparative study of ozonation, iron coated zeolite catalyzed ozonation and granular activated carbon catalyzed ozonation of humic acid. *Chemosphere.* 2017;174:218–231.
- [55] Rodríguez FJ, Schlenger P, García-Valverde M. Monitoring changes in the structure and properties of humic substances following ozonation using UV-Vis, FTIR and ¹H NMR techniques. *Sci Total Environ.* 2016;541:623–637.
- [56] Vicente F, Rosas JM, Santos A, et al. Improvement soil remediation by using stabilizers and chelating agents in a Fenton-like process. *Chem Eng J.* 2011;172:689–697.
- [57] Romero A, Santos A, Vicente F. Chemical oxidation of 2,4-dimethylphenol in soil by heterogeneous Fenton process. *J Hazard Mater.* 2009;162:785–790.
- [58] HACH. HACH DR/890 Procedures Manual. HACH Company; 2013. p. 7–613.
- [59] Favoretto E. EFLUENTES E ÁGUAS DIVERSAS. RESIDUAL DE H₂O₂ - LA0-MA-057/15 (v. 2.0). Curitiba, Paraná; 2015.
- [60] Santos N de O dos. Estudo do Processo Oxidativo Avançado FZV / H₂O₂ para a pré-oxidação da matéria orgânica natural em águas de superfície. Doctoral thesis. Department of Chemical and Materials Engineering. PUC RIO; 2019.
- [61] Dubowski Y, Greenberg-Eitan R, Rebhun M. Removal of Trihalomethane Precursors by Nanofiltration in Low-SUVA Drinking Water. *Water.* 2018;10:1370.
- [62] Sloboda E, Vieira EM, Dantas ADB, et al. Influência das características das substâncias

- húmicas aquáticas na eficiência da coagulação com o cloreto férrico. *Quim Nova*. 2009;32:976–982.
- [63] Li A-N, Li S, Zhang Y-J, et al. Resources and Biological Activities of Natural Polyphenols. *Nutrients* [Internet]. 2014;6:6020–6047. Available from: <http://www.mdpi.com/2072-6643/6/12/6020>.
- [64] Brglez Mojzer E, Knez Hrnčič M, Škerget M, et al. Polyphenols: Extraction Methods, Antioxidative Action, Bioavailability and Anticarcinogenic Effects. *Molecules* [Internet]. 2016;21:901. Available from: <http://www.mdpi.com/1420-3049/21/7/901>.
- [65] Lu J, Zhang T, Ma J, et al. Evaluation of disinfection by-products formation during chlorination and chloramination of dissolved natural organic matter fractions isolated from a filtered river water. *J Hazard Mater*. 2009;162:140–145.
- [66] Mohd Zainudin F, Abu Hasan H, Sheikh Abdullah SR. An overview of the technology used to remove trihalomethane (THM), trihalomethane precursors, and trihalomethane formation potential (THMFP) from water and wastewater. *J Ind Eng Chem* [Internet]. 2018;57:1–14. Available from: <https://linkinghub.elsevier.com/retrieve/pii/S1226086X17304410>.
- [67] Sarathy SR, Stefan MI, Royce A, et al. Pilot-scale UV/H₂O₂ advanced oxidation process for surface water treatment and downstream biological treatment: effects on natural organic matter characteristics and DBP formation potential. *Environ Technol*. 2011;32:1709–1718.
- [68] Kitis M, Karanfil T, Kilduff JE, et al. The reactivity of natural organic matter to disinfection by-products formation and its relation to specific ultraviolet absorbance. *Water Sci Technol*. 2001;43:9–16.
- [69] Wu Y, Zhou S, Ye X, et al. Oxidation and coagulation removal of humic acid using Fenton process. *Colloids Surfaces A Physicochem Eng Asp*. 2011;379:151–156.
- [70] Zhong X, Cui C, Yu S. Identification of Oxidation Intermediates in Humic Acid Oxidation. *Ozone Sci Eng*. 2018;40:93–104.
- [71] Huang Z, Gu Z, Wang Y, et al. Improved oxidation of refractory organics in

- concentrated leachate by a Fe²⁺-enhanced O₃/H₂O₂ process. *Environ Sci Pollut Res.* 2019;
- [72] Menon P, Anantha Singh TS, Pani N, et al. Electro-Fenton assisted sonication for removal of ammoniacal nitrogen and organic matter from dye intermediate industrial wastewater. *Chemosphere.* 2021;269:128739.
- [73] Nidheesh PV, Gandhimathi R. Comparative Removal of Rhodamine B from Aqueous Solution by Electro-Fenton and Electro-Fenton-Like Processes. *CLEAN - Soil, Air, Water.* 2014;42:779–784.
- [74] Santos-Juanes L, García-Ballesteros S, Vercher RF, et al. Commercial steel wool used for Zero Valent Iron and as a source of dissolved iron in a combined red-ox process for pentachlorophenol degradation in tap water. *Catal Today.* 2019;328:252–258.
- [75] Dong J, Zhao Y, Zhao R, et al. Effects of pH and particle size on kinetics of nitrobenzene reduction by zero-valent iron. *J Environ Sci.* 2010;22:1741–1747.
- [76] Kallel M, Belaid C, Boussahel R, et al. Olive mill wastewater degradation by Fenton oxidation with zero-valent iron and hydrogen peroxide. *J Hazard Mater.* 2009;163:550–554.
- [77] Jun L, Qingqing J, Bo L, et al. Optimization , performance and mechanisms. *J Taiwan Inst Chem Eng [Internet].* 2017;0:1–9. Available from:
<http://dx.doi.org/10.1016/j.jtice.2017.09.002>.
- [78] Kang S-H, Choi W. Oxidative Degradation of Organic Compounds Using Zero-Valent Iron in the Presence of Natural Organic Matter Serving as an Electron Shuttle. *Environ Sci Technol [Internet].* 2009;43:878–883. Available from:
<https://pubs.acs.org/doi/10.1021/es900076m>.
- [79] Malik PK, Saha SK. Oxidation of direct dyes with hydrogen peroxide using ferrous ion as catalyst. *Sep Purif Technol.* 2003;31:241–250.
- [80] Fischbacher A, Sonntag C von, Schmidt TC. Hydroxyl radical yields in the Fenton process under various pH, ligand concentrations and hydrogen peroxide/Fe(II) ratios. *Chemosphere.* 2017;182:738–744.

- [81] Ertugay N, Kocakaplan N, Malkoç E. Investigation of pH effect by Fenton-like oxidation with ZVI in treatment of the landfill leachate. *Int J Mining, Reclam Environ.* 2017;31:404–411.
- [82] Pourbaix M. *Atlas of Chemical and Electrochemical Equilibria in Aqueous Solution*. 2nd ed. National Association of Corrosion Engineers 1974, editor. Natl. Assoc. Corros. Eng. Houston, Texas, USA; 1974.
- [83] Bowes MJ, Armstrong LK, Harman SA, et al. Weekly water quality monitoring data for the River Thames (UK) and its major tributaries (2009–2013): the Thames Initiative research platform. *Earth Syst Sci Data.* 2018;10:1637–1653.
- [84] Hanamoto S, Nakada N, Jürgens MD, et al. The different fate of antibiotics in the Thames River, UK, and the Katsura River, Japan. *Environ Sci Pollut Res.* 2018;25:1903–1913.
- [85] London CO, Services E. *Thames River Water Quality 2016*. London; 2017.
- [86] Wang G-S, Hsieh S-T. Monitoring natural organic matter in water with scanning spectrophotometer. *Environ Int.* 2001;26:205–212.
- [87] Munro K, Martins CPB, Loewenthal M, et al. Evaluation of combined sewer overflow impacts on short-term pharmaceutical and illicit drug occurrence in a heavily urbanised tidal river catchment (London, UK). *Sci Total Environ* [Internet]. 2019;657:1099–1111. Available from: papers2://publication/uuid/3652883C-4F63-413F-9414-7E361176E64C.
- [88] Xu L, Campos LC, Li J, et al. Removal of antibiotics in sand, GAC, GAC sandwich and anthracite/sand biofiltration systems. *Chemosphere.* 2021;275:130004.
- [89] Pifer AD, Fairey JL. Improving on SUVA₂₅₄ using fluorescence-PARAFAC analysis and asymmetric flow-field flow fractionation for assessing disinfection byproduct formation and control. *Water Res.* 2012;46:2927–2936.
- [90] Nagoya S, Nakamichi S, Kawase Y. Mechanisms of phosphate removal from aqueous solution by zero-valent iron: A novel kinetic model for electrostatic adsorption, surface complexation and precipitation of phosphate under oxic conditions. *Sep Purif Technol* [Internet]. 2019;218:120–129. Available from:

<https://linkinghub.elsevier.com/retrieve/pii/S1383586618341509>.

- [91] Sleiman N, Deluchat V, Wazne M, et al. Phosphate removal from aqueous solutions using zero valent iron (ZVI): Influence of solution composition and ZVI aging. *Colloids Surfaces A Physicochem Eng Asp.* 2017;514:1–10.
- [92] Ruales-Lonfat C, Barona JF, Sienkiewicz A, et al. Iron oxides semiconductors are efficient for solar water disinfection: A comparison with photo-Fenton processes at neutral pH. *Appl Catal B Environ.* 2015;166–167:497–508.
- [93] Giannakis S, Polo López MI, Spuhler D, et al. Solar disinfection is an augmentable, in situ -generated photo-Fenton reaction—Part 1: A review of the mechanisms and the fundamental aspects of the process. *Appl Catal B Environ.* 2016;199:199–223.
- [94] Xiang W, Zhang B, Zhou T, et al. An insight in magnetic field enhanced zero-valent iron/H₂O₂ Fenton-like systems: Critical role and evolution of the pristine iron oxides layer. *Sci Rep.* 2016;6:1–11.
- [95] Ling R, Chen JP, Shao J, et al. Degradation of organic compounds during the corrosion of ZVI by hydrogen peroxide at neutral pH: Kinetics, mechanisms and effect of corrosion promoting and inhibiting ions. *Water Res.* 2018;134:44–53.
- [96] Ma Q, Cui L, Zhou S, et al. Iron nanoparticles in situ encapsulated in lignin-derived hydrochar as an effective catalyst for phenol removal. *Environ Sci Pollut Res.* 2018;25:20833–20840.
- [97] Zhang M, Li J, Wang Y, et al. Impacts of different biochar types on the anaerobic digestion of sewage sludge. *RSC Adv.* 2019;9:42375–42386.
- [98] Li J, Ji Q, Lai B, et al. Degradation of p -nitrophenol by Fe⁰/H₂O₂/persulfate system: Optimization, performance and mechanisms. *J Taiwan Inst Chem Eng.* 2017;80:686–694.
- [99] Liu A, Liu J, Pan B, et al. Formation of lepidocrocite (γ -FeOOH) from oxidation of nanoscale zero-valent iron (nZVI) in oxygenated water. *RSC Adv.* 2014;4:57377–57382.
- [100] Landolt D. *Corrosion and Surface Chemistry of Metals*. First Ed. EPFL Press, editor. Lausanne; 2007.

- [101] Cabrera Reina A, Miralles-Cuevas S, Casas López JL, et al. Pyrimethanil degradation by photo-Fenton process: Influence of iron and irradiance level on treatment cost. *Sci Total Environ* [Internet]. 2017;605–606:230–237. Available from: <https://linkinghub.elsevier.com/retrieve/pii/S0048969717316376>.
- [102] Rodrigues CSD, Madeira LM, Boaventura RAR. Optimization and Economic Analysis of Textile Wastewater Treatment by Photo-Fenton Process under Artificial and Simulated Solar Radiation. *Ind Eng Chem Res* [Internet]. 2013;52:13313–13324. Available from: <https://pubs.acs.org/doi/10.1021/ie401301h>.
- [103] Carra I, Ortega-Gómez E, Santos-Juanes L, et al. Cost analysis of different hydrogen peroxide supply strategies in the solar photo-Fenton process. *Chem Eng J* [Internet]. 2013;224:75–81. Available from: <https://linkinghub.elsevier.com/retrieve/pii/S1385894712012582>.
- [104] Ribeiro JP, Marques CC, Portugal I, et al. Fenton processes for AOX removal from a kraft pulp bleaching industrial wastewater: Optimisation of operating conditions and cost assessment. *J Environ Chem Eng* [Internet]. 2020;8:104032. Available from: <https://linkinghub.elsevier.com/retrieve/pii/S2213343720303808>.
- [105] Central de Ferramentas, Caixas RJ [Internet]. 2021 [cited 2021 Mar 18]. p. 1–6. Available from: <https://www.centraldeferramentas.com.br/Produto/prego-c-c-12x12-gerdau-7785.10005>.
- [106] Kauri - casa do marceneiro [Internet]. 2021. p. 1–6. Available from: <https://www.kaury.com.br/prego-12x12-com-cabeca-1kg-arcelor-mittal#.YFacwJ1KjIV>.
- [107] Trade Fix direct [Internet]. 2021 [cited 2021 Mar 18]. Available from: <https://tradefixdirect.com/stainless-steel-nails/stainless-steel-a2304-annular-ring-nails-25-x-265mm%0A%0A>.
- [108] Anderson W. United States Patent Office [Internet]. Google Patents. England; 1885. p. 131–134. Available from: <https://dl.acm.org/doi/10.1145/178951.178972>.

Appendix A. Supplementary data

Table A. 1 – Sample dataset collected for Regent's Park lake water during the Summer (RWS) and Autumn (RWA) seasons.

Sample	Day	Month	T (°C)	Precipitation (mm)	pH	DOC (mg L ⁻¹)	UV ₂₅₄	SUVA ₂₅₄ (L mg ⁻¹ m ⁻¹)
RWS-1	25	7	25.5	0.0	8.4	7.3 ±0.2	0.164	2.246
RWS-2	21	8	25.5	0.05	8.5	2.65 ±0.03	0.033 ±0.001	1.245
RWS-3	28	8	22.0	0.0	8.4	2.8 ±0.28	0.065 ±0.001	2.321
RWS-4	5	9	25	0.0	8.4	3.7 ±0.25	0.063 ±0.007	1.703
RWS-5	10	9	24.5	0.0	8.2	2.24 ±0.02	0.050 ± 0.000	2.232
RWS-6	17	9	25	0.0	8.4	3.64 ±0.25	0.077 ±0.000	2.115
RWA-7	3	10	23	0.0	8.3	5 ±0.012	0.122 ±0.007	2.440
RWA-8	8	10	21	0.0	7.7	5 ±0.03	0.135 ± 0.0015	2.700
RWA-9	15	10	18.6	0.0	7.7	5.8 ±0.113	0.155 ±0.007	2.672
RWA-10	18	10	21.6	0.0	7.8	5.76 ±0.03	0.153 ±0.007	2.684
RWA-11	2	11	22	0.0	7.9	7.15 ±0.14	0.161 ±0.007	2.252
RWA-12	12	11	19	1.14	7.9	6.75 ±0.184	0.176 ±0.007	2.607
RWA-13	20	11	18	3.1	7.7	6.6 ±0.2	0.184 ±0.001	2.787

Table A.2 - Chemical composition of ZVI nail obtained by optical emission spectroscopy (OES).

Elements	C	Si	Mn	P	S	Cr	Ni	Mo
Concentration (mass %)	0.13	0.15	0.59	0.027	0.016	0.05	0.03	< 0.01

Table A.3 – Instruments used for the determination of general water quality parameters.

Analysis	Instrument
<i>ZVI-nail characterization</i>	
Optical Emission Spectroscopy	Spectromax Instrument
Scanning electron microscopes	(FEGSEM) (JEOL JSM 7100F) - Oxford Instruments Detector 80 windowless silicon drift detector (SDD)
X-ray photoelectron spectroscopy (XPS)	Spectrometer Thermo K-alpha (E = 1486.6 eV)
<i>Organic matter characterization</i>	
Dissolved Organic Carbon	TOC-L Shimadzu model, TOC analyzer
UV absorbance (254 nm)	Shimadzu UV 1800, spectrophotometer
<i>Ion characterization</i>	
nitrate, chloride, phosphate, bromide	IC1100, Dionex
Total iron	Varian - ICP-AES, 720-ES
Ferrous iron	HACH 890 colorimeter
Hydrogen peroxide	HACH 890 colorimeter
Dissolved oxygen	Jenway 9200
Chlorine	HACH DR300 colorimeter
pH and Temperature	Mettler Toledo, S47K
Turbidity	HACH 2100AN IS turbidmeter
Conductivity	Mettler Toledo, S47K
Jar Tester-Lab, Phipps & Bird, 7790-950	

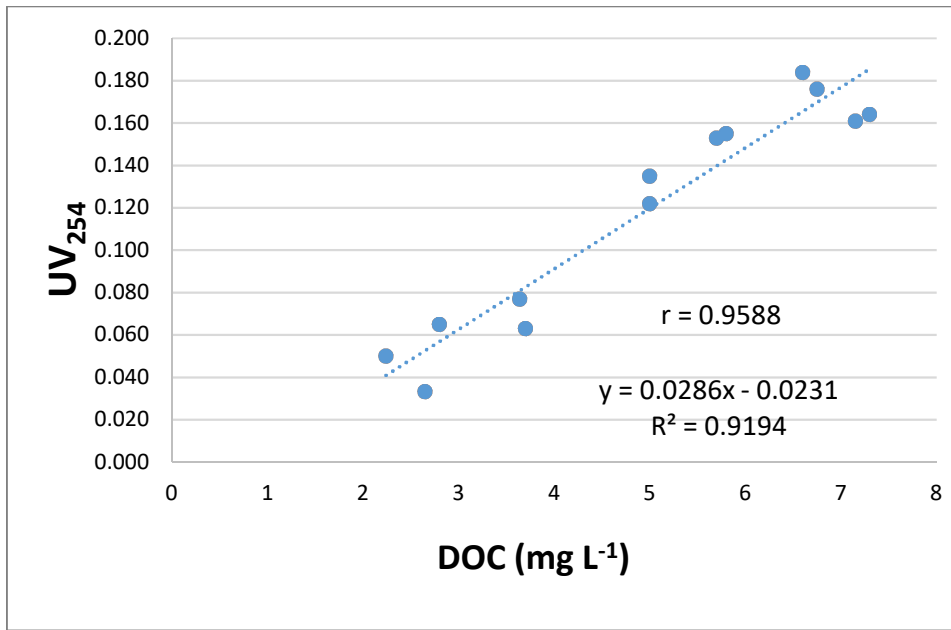
Table A.4 – DOC and UV₂₅₄ removals from the treatments: ZVI/H₂O₂, only ZVI, and only H₂O₂. The experiments were carried out with samples collected during the Autumn season.

Treatment	Experimental Condition	Sample Identification	DOC - Removal (%)	UV ₂₅₄ -Removal (%)	Observations
ZVI/H ₂ O ₂	H ₂ O ₂ =1.5 times the stoichiometric amount; pH=5.5; ZVI=37.5 g L ⁻¹	RWA-9.1	31.16	72	
ZVI/H ₂ O ₂	H ₂ O ₂ =1.5 times the stoichiometric amount; pH=5.5; ZVI=37.5 g L ⁻¹	RWA-9.2	26.3	67.84	
ZVI/H ₂ O ₂	H ₂ O ₂ =1.5 times the stoichiometric amount; pH=5.5; ZVI=37.5 g L ⁻¹	RWA-9.3	33.77	63.22	
ZVI	H ₂ O ₂ =1.5 times the stoichiometric amount; pH=5.5; ZVI=37.5 g L ⁻¹	RWA-10.1	21.96	20.78	
ZVI	H ₂ O ₂ =1.5 times the stoichiometric amount; pH=5.5; ZVI=37.5 g L ⁻¹	RWA-10.2	18.49	-	
H ₂ O ₂	H ₂ O ₂ =1.5 times the stoichiometric amount; pH=5.5; ZVI=37.5 g L ⁻¹	RWA-10.3	0	-	
H ₂ O ₂	H ₂ O ₂ =1.5 times the stoichiometric amount; pH=5.5; ZVI=37.5 g L ⁻¹	RWA-10.4	0	-	
ZVI/H ₂ O ₂	H ₂ O ₂ =2 times the stoichiometric amount; pH=3.5; ZVI=50 g L ⁻¹	RWA-12.1	64.7	84.1	1 ^o cycle of nail-ZVI use
ZVI/H ₂ O ₂	H ₂ O ₂ =2 times the stoichiometric amount; pH=3.5; ZVI=50 g L ⁻¹	RWA-12.2	58.27	76	1 ^o cycle of nail-ZVI use
ZVI/H ₂ O ₂	H ₂ O ₂ =2 times the stoichiometric amount; pH=3.5; ZVI=50 g L ⁻¹	RWA-12.3	55.5	72	1 ^o cycle of nail-ZVI use
ZVI/H ₂ O ₂	H ₂ O ₂ =2 times the stoichiometric amount; pH=3.5; ZVI=50 g L ⁻¹	RWA-12.4	-	64.56	2 ^o cycle of nail-ZVI use
ZVI/H ₂ O ₂	H ₂ O ₂ =2 times the stoichiometric amount; pH=3.5; ZVI=50 g L ⁻¹	RWA-12.5	-	68	2 ^o cycle of nail-ZVI use
ZVI/H ₂ O ₂	H ₂ O ₂ =2 times the stoichiometric amount; pH=3.5; ZVI=50 g L ⁻¹	RWA-12.6	44.98	57.7	3 ^o cycle of nail-ZVI use
ZVI/H ₂ O ₂	H ₂ O ₂ =2 times the stoichiometric amount; pH=3.5; ZVI=50 g L ⁻¹	RWA-12.7	38	62.5	3 ^o cycle of nail-ZVI use
ZVI/H ₂ O ₂	H ₂ O ₂ =2 times the stoichiometric amount; pH=3.5; ZVI=50 g L ⁻¹	RWA-12.8	42	57	4 ^o cycle of nail-ZVI use
ZVI/H ₂ O ₂	H ₂ O ₂ =2 times the stoichiometric amount; pH=3.5; ZVI=50 g L ⁻¹	RWA-12.9	34	64.2	4 ^o cycle of nail-ZVI use
ZVI/H ₂ O ₂	H ₂ O ₂ =2 times the stoichiometric amount; pH=3.5; ZVI=50 g L ⁻¹	TWA-1.1	57.4	79.8	
ZVI/H ₂ O ₂	H ₂ O ₂ =2 times the stoichiometric amount; pH=3.5; ZVI=50 g L ⁻¹	TWA-1.2	64.2	80.6	
ZVI/H ₂ O ₂	H ₂ O ₂ =2 times the stoichiometric amount; pH=3.5; ZVI=50 g L ⁻¹	TWA-1.3	63.2	79.4	

RWA = Regent's Park water collected during Autumn season.

TWA = River Thames water collected during Autumn season.

1



2

3 **Figure A.1** – Relationship between UV₂₅₄ and DOC values in natural water samples
4 collected from Regent's Park lake during the Summer and Autumn seasons ($R^2 =$
5 determination coefficient and $r =$ Pearson value).

6

7

8 **Table A.5** – DOC removals by the ZVI/H₂O₂ process, only ZVI nail, and only H₂O₂ in
 9 Regent’s Park lake water (during the Autumn – RWA). Experimental conditions: H₂O₂ =
 10 1.5 times the stoichiometric amount, pH₀ = 5.5, ZVI = 37.5 g L⁻¹. ZVI/H₂O₂ treatment
 11 applied in samples RWA-9, n=3 (9.1; 9.2; 9.3). Only ZVI applied in samples RWA-10.1
 12 and RWA-10.2). Only H₂O₂ applied in samples RWA-10.3 and RWA-10.4.

	DOC removal (%) ZVI/H ₂ O ₂			DOC removal (%) Only ZVI		DOC removal (%) Only H ₂ O ₂	
Time (min)	RWA- 9.1	RWA- 9.2	RWA- 9.3	RWA- 10.1	RWA- 10.2	RWA- 10.3	RWA- 10.4
0	0	0	0	0	0	0	0
15	23.14	24.82	22.74	0	0	0	0.224
30	28.7	23.2	32.24	5.95	3.73	0	0
60	29.73	26.6	29.54	8.046	8.34	0	0
120	33.77	26.3	31.16	18.49	21.96	0	0

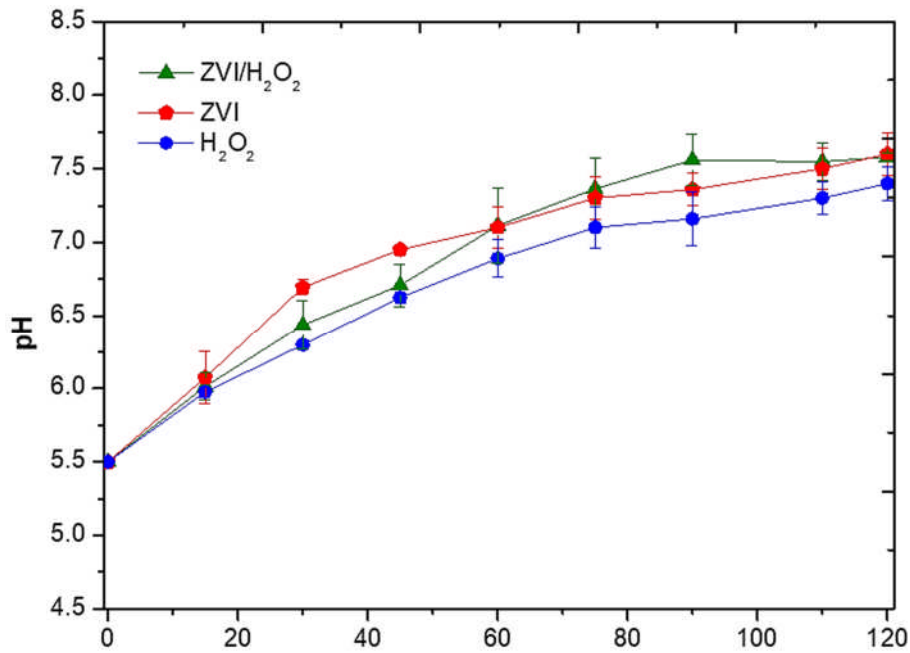
13

14

15

16

17



18

19 **Figure A.2** - Behaviour of pH in Regent's Park lake during the processes: (a) ZVI/H₂O₂,
 20 (b) only ZVI, and (c) only H₂O₂. Experimental conditions: pH₀ = 3.5, [H₂O₂]₀ = 2 times
 21 the stoichiometric amount, and ZVI = 50 g L⁻¹. Experimental conditions: H₂O₂ = 1.5 times
 22 the stoichiometric amount, pH₀ = 5.5, ZVI = 37.5 g L⁻¹. ZVI/H₂O₂ treatment applied in
 23 samples RWA-9.1, RWA-9.2 and RWA-9.3. Only ZVI applied in samples RWA-10.1
 24 and RWA-10.2. Only H₂O₂ applied in samples RWA-10.3 and RWA-10.4.

25

26

27

28

29

30

31

32 **Table A.6** - Pseudo-first order kinetics and second order kinetic coefficient for DOC
 33 removal in the processes with ZVI/H₂O₂ and only ZVI.

Process	Pseudo- first order		Pseudo- second order	
	K ₁ (min ⁻¹)	R ²	K ₂ (L mg ⁻¹ min ⁻¹)	R ²
ZVI/H ₂ O ₂	0.0021	0.4631	0.0005	0.4919
Only ZVI	0.002	0.9347	0.0004	0.9404

34

35

36

37

38

39

40

41

42

43

44

45

46

47

48

49

50 **Table A.7** - Average and standard deviation of the composition characteristics of natural
 51 water obtained from Regent's Park lake and the Thames river.

Parameters	Unit	Regent's Park lake	Thames river (n = 3)
------------	------	-----------------------	-------------------------

		(n = 5)	Mean ± SD
		Mean ± SD	
UV₂₅₄	cm ⁻¹	0.175 ± 0.01	0.138 ± 0.03
* SUVA	L mg ⁻¹ m ⁻¹	2.3 ± 0.70	2.01 ± 0.87
pH		7.76 ± 0.1	7.4 ± 0.14
**DOC	mg L ⁻¹	8.12 ± 2.5	7.17 ± 1.59
Dissolved Oxygen	mg L ⁻¹	3.43 (19 °C) ±0.43	5.15 (17.4°C)
Turbidity	NTU	1.22 ± 0.25	13.1 ± 0.01
Conductivity	µS cm ⁻¹	1008 ± 38.42	n.a.
Chlorine (free)	mg L ⁻¹	0.03 ± 0.01	0.09
Iron (total)	mg L ⁻¹	0.024 ± 0.004	n.a.
Chloride	mg L ⁻¹	76.95 ± 1.29	539.8 ± 0.01
Nitrate	mg L ⁻¹	1.31 ± 0.97	45.5 ± 0.02
Bromide	mg L ⁻¹	0.21 ± 0.04	1.34 ± 0.01

52 *SUVA: specific ultraviolet absorbance ($SUVA_{\lambda} = UV_{\lambda} / COD * 100$, where λ is the specific wavelength).

53 **DOC: Dissolved Organic Carbon. Results of natural water obtained from collections in autumn.

54 n.a. = not analyzed

55 Samples from Regent's Park lake: minimum and maximum values (mg L⁻¹), respectively: UV₂₅₄ 0.161 –

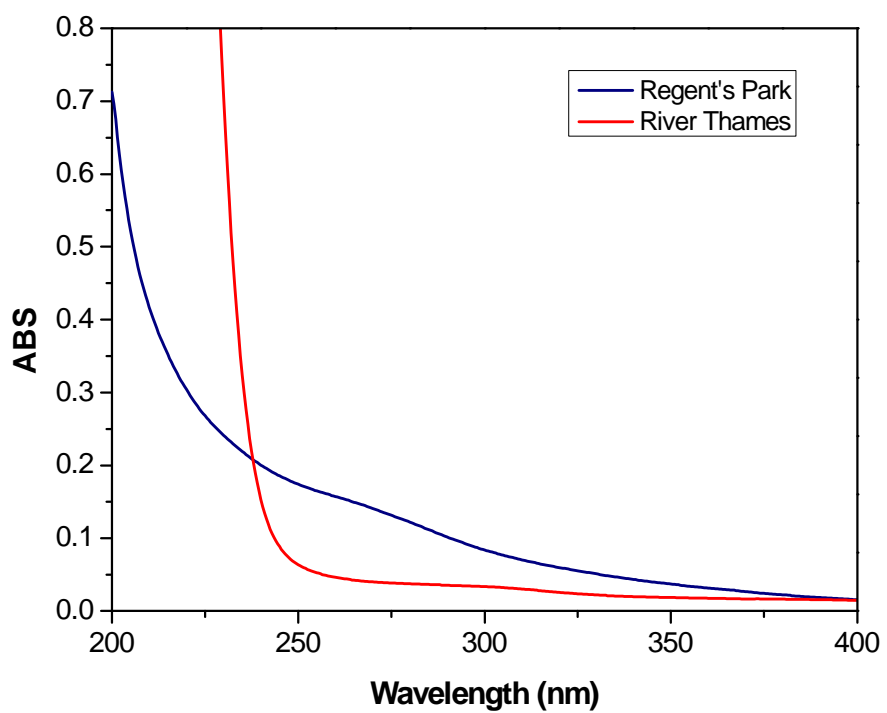
56 0.184 (median: 0.168); DOC 6.6 – 11 (median: 7.14); pH 7.56 – 7.95 (median: 7.75); Dissolved Oxygen

57 3.13 – 3.74 (median: 3.4); Turbidity 0.98 – 1.47 (median: 1.22); Conductivity 976 – 1050 (median: 982);

58 Chlorine 0.02 – 0.041 (median: 0.02); Chloride 75.3 – 79.8 (median: 75.8) ; Nitrate 0.3 - 2.6 (median: 1.4);

59 Bromide 0.17 – 0.24 (median: 0.21).

60



61

62 **Figure A.3** - UV-Vis spectra for Regent's Park lake and the Thames river water samples

63 before ZVI/H₂O₂ process. The spectrum results refer to samples collected at the same

64 day.

65

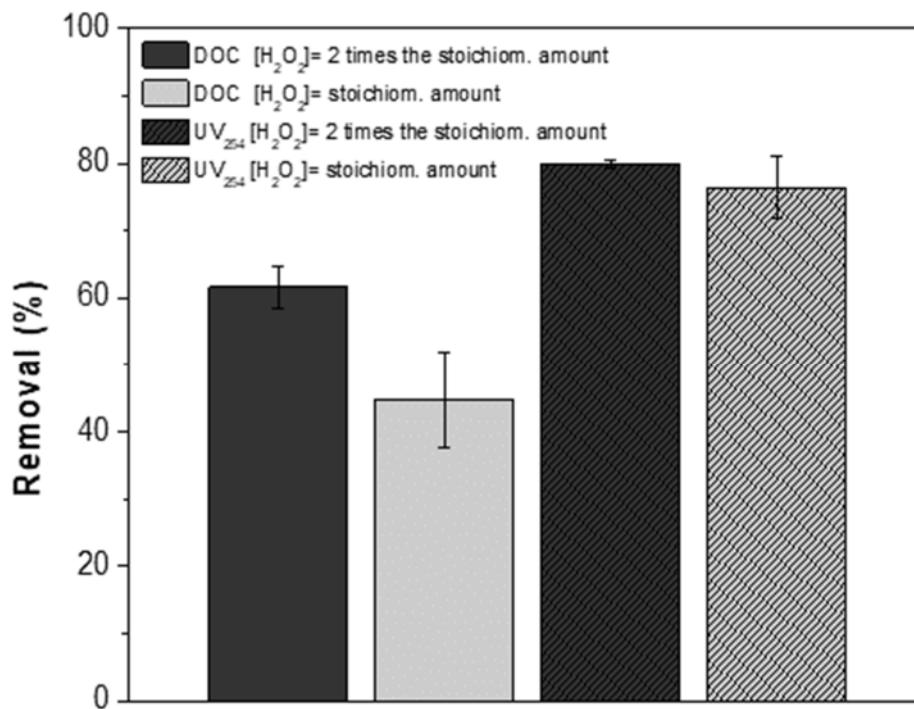
66

67

68

69

70



71

72 **Figure A.4** - Removal of NOM by parameters DOC and UV₂₅₄ through the ZVI/H₂O₂
 73 process applied in the Thames river water samples after varying the initial dosages of
 74 H₂O₂. Experimental conditions: pH₀ = 3.5, ZVI nail = 50 g L⁻¹, and [H₂O₂] =
 75 stoichiometric amount) and 2 times the stoichiometric amount).

76

77

78

79 **Equation A.1**

80
$$\ln ([\text{H}_2\text{O}_2]_t / [\text{H}_2\text{O}_2]_0) = -k_{\text{H}_2\text{O}_2} \cdot t \quad (\text{A.1})$$

81 Calculations of the pseudo-first order constants of the H₂O₂ concentration decay.

82 where: $k_{\text{H}_2\text{O}_2}$ is the velocity constant for the H₂O₂ decay reaction during the ZVI/H₂O₂

83 process at a given time (t).

84

85

86

87

88

89

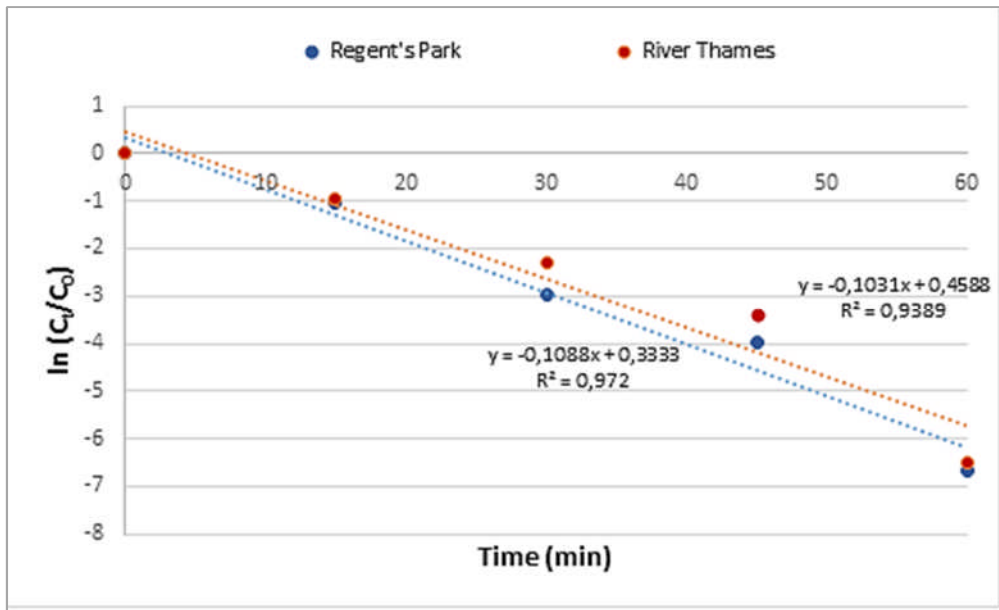
90

91

92

93

94



95

96 **Figure A.5** - H₂O₂ consumption in the ZVI/H₂O₂ reaction applied to water samples from
 97 Regent's Park lake and the Thames river. The adjustment for the pseudo-first-order
 98 reaction model indicated R² = 0.972 and R² = 0.9389 for water from Regent's Park and
 99 Thames river, respectively. Experimental conditions: pH₀ = 3.5, [H₂O₂]₀ = 2 times the
 100 stoichiometric amount), and ZVI nail = 50 g L⁻¹.

101

102

103

104 **Table A.8** - Concentrations of chloride, nitrate, bromide and phosphate in the Thames
 105 river and Regent's Park lake water samples before and after ZVI/H₂O₂ process.
 106 Experimental conditions: pH₀ = 3.5, [H₂O₂]₀ = 2 times the stoichiometric amount, and
 107 ZVI nail = 50 g L⁻¹.

108

Concentration (mg L ⁻¹)	Thames river		Regent's Park lake	
	time = 0 min	time = 60 min	time = 0 min	time = 60 min
Chloride	540 ± 4.9	506.7 ± 5.8	73.9 ± 2.73	62.2 ± 1.7
Nitrate	45 ± 0.42	38.9 ± 0.15	2.35 ± 0.28	1.95 ± 0.07
Bromide	1.35 ± 0.04	1.14 ± 0.06	0.24 ± 0.01	0.21 ± 0.01
Phosphate	1.85 ± 0.05	0	1.15 ± 0.21	0

109

110

111

112

113

114

115

116

117

118

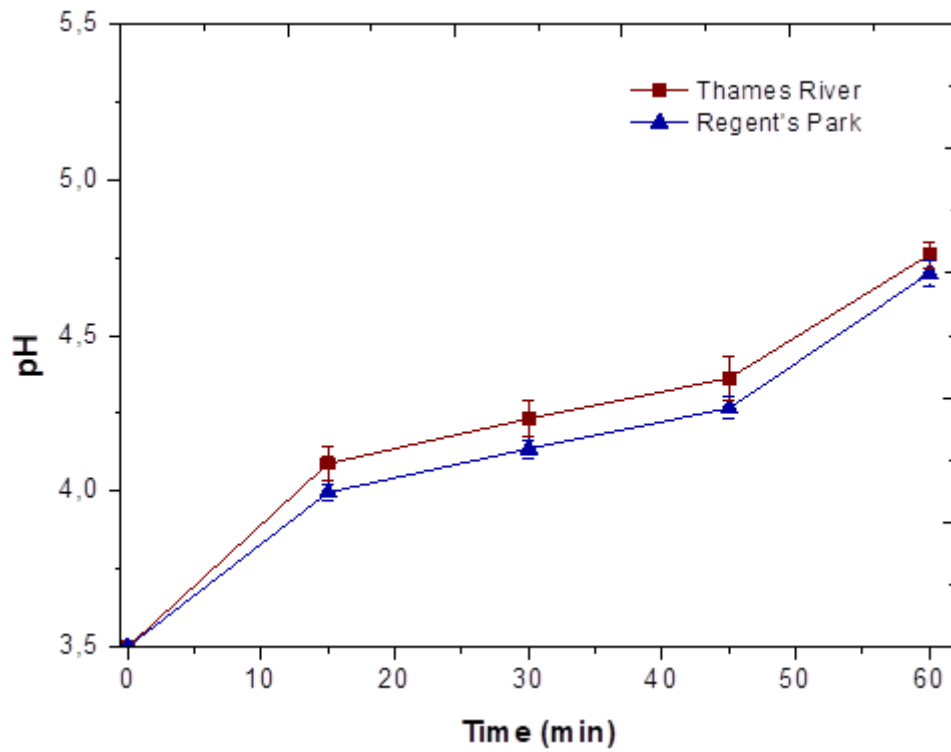
119

120

121

122

123



125

126 **Figure A.6** - Behaviour of pH in Regent's Park lake and Thames river water samples'
 127 during the ZVI/H₂O₂ process. Experimental conditions: pH₀ = 3.5, [H₂O₂]₀ = 2 times the
 128 stoichiometric amount, and ZVI = 50 g L⁻¹.

129

130

131

132

133

134

135

136

137

138

139

140

141

142

143

144

145

146

147

148

149

150

151

152

153

154

155

156

157

158